JOURNAL OF MATERIALS SCIENCE 20 (1985) 3041 – 3073

Review
Subcritical crack growth, surface energy, fracture toughness, stick–slip and embrittlement

D. MAUGIS
Equipe de Recherche ER 259, Mécanique des Surfaces CNRS, Laboratoire Central des Ponts et Chaussées, 58 Bd Lefebvre, 75015 Paris, France

It is proposed that the difficulties encountered with the meaning of subcritical crack growth arose from a misunderstanding of the Griffith equation. This equation is $G = 2\gamma$ for an equilibrium crack (stable or unstable) where γ is the intrinsic surface energy. When $G > 2\gamma$ the crack has a velocity v depending on the crack extension force $G - 2\gamma$, even in a vacuum, and the following equation, well verified for adherence of elastomers,

$$G - 2\gamma = 2\gamma\phi_T(v)$$

where $\phi_T(v)$ is related to viscoelastic losses or internal friction at the crack tip, is generalized to other materials. At a critical speed v_c, $d\phi/dv$ becomes negative; as a negative branch cannot be observed the velocity jumps to high values on a second positive branch, so that $G = G_c$ is a criterion for crack speed discontinuity, not the Griffith criterion. The multiplicative factor 2γ on the right-hand side accounts for the shift of the v–K curves with environment. No stress corrosion is needed to explain subcritical crack growth. Subcritical crack growth in glasses and ceramics and velocity jump in brittle polymers are shown to agree with this proposal. This model can also explain stick–slip motion when a mean velocity is imposed in the negative branch. Occurrence of velocity jump or stick–slip depends on the geometry tested and the stiffness of the apparatus. A second kind of stick–slip associated with cavitation in liquid-filled cracks is discussed. When the surrounding medium can reach the crack tip and reduce the surface energy, even at the critical speed v_c, the critical strain energy release rate G_c is reduced in the same proportion as γ, and a loading which would have given subcritical growth will give a catastrophic failure. Reduction of surface energy in the Rehbinder effect and in embrittlement by segregation is discussed. Finally, the evolution of ideas concerning the Irwin–Orowan formula and fracture toughness is examined.

1. Introduction

Adherence of solids, mechanics of contact and fracture mechanics are three facets of the same object [1], and progress in one field can enlighten the others. This papers has its origin in the work of Maugis and Barquins on the adhesive contact of axisymmetric punches on rubbers [2–5]. Following the work of Johnson, Kendall and Roberts (JKR) [6] on the contact of elastic solids with surface energy, it was soon recognized that the calculation of radius of contact was that of Griffith's criterion, the edge of

0022–2461/85 $03.00 + .12

the contact area being viewed as a crack propagating at the interface. Maugis and Barquins studied such equilibrium cracks, crack healing and the kinetics of crack propagation at fixed load, fixed grips and fixed cross-head velocity. They proposed an equation for kinetics of crack propagation, taking into account the effect of environment, and Maugis [7] discussed the meaning of G_c and K_c for such viscoelastic solids. This paper is a tentative attempt to generalize this view to other solids such as glasses, ceramics, brittle polymers and metals.

2. The Griffith criterion

Let us consider the system made of two elastic solids in contact over an area A. This system can exchange work and heat, but not matter, with the exterior. A force P (compressive or tensile) can be applied on the two elastic bodies, either by a dead load as in Fig. 1a, or by a spring of stiffness k_m as in Fig. 1b. The area of contact is allowed to vary at fixed load P, or at fixed displacement for k_m infinite (or more generally at fixed displacement Δ), so that the state of the system depends in general on two independent variables P, A or δ, A. The edge of the contact area can be considered as an interface crack tip in Mode I that recedes or advances as the area of contact increases or decreases. We will neglect any interfacial shear stress so that the system is the same as for a notched solid, but with an imposed crack path.

The energy of the system $U = U(S, \delta, A)$ is a function of the extensive variables S (entropy), δ, A; it can be decomposed into elastic energy U_E and interface energy $U_S = -wA$, where $w = \gamma_1 + \gamma_2 - \gamma_{12}$ is the Dupré energy of adhesion, a material property independent of crack velocity which replaces the intrinsic surface energy 2γ at an interface. The first differential of the energy can be written in the form

$$dU = TdS + Pd\delta + (G - w)dA \quad (1)$$

with

$$\left(\frac{\partial U}{\partial S}\right)_{\delta,A} = T$$

$$\left(\frac{\partial U}{\partial \delta}\right)_{S,A} = \left(\frac{\partial U_E}{\partial \delta}\right)_{S,A} = P$$

$$\left(\frac{\partial U}{\partial A}\right)_{S,\delta} = \left(\frac{\partial U_E}{\partial A}\right)_{S,\delta} + \left(\frac{\partial U_S}{\partial A}\right)_{S,\delta} = G - w$$

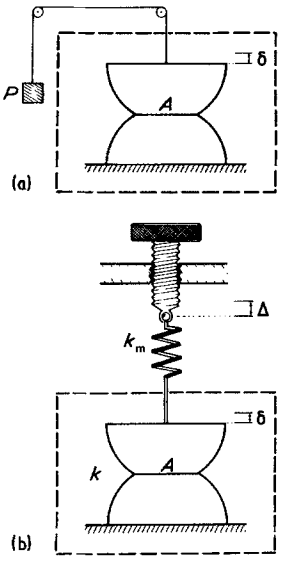

Figure 1 Equilibrium contact of two elastic solids: (a) dead load, (b) testing machine with finite stiffness k_m.

G, which describes the variation of elastic energy with A, at constant δ, is the strain energy release rate. Note that wA is considered here as a kind of potential energy which can be recovered by crack healing. The three relationships

$$T = T(\delta, A, S) \quad (2a)$$

$$P = P(\delta, A, S) \quad (2b)$$

$$G = G(\delta, A, S) \quad (2c)$$

expressing intensive parameters in terms of the independent extensive parameters, are the *equations of state* of the system. Knowledge of these three equations of state is equivalent to knowledge of the fundamental equation $U = U(S, \delta, A)$, and gives a thermodynamically complete description of the system.

A system is in equilibrium if virtual perturbations of the extensive variables leave its energy constant. However, equilibrium is often studied in the presence of constraints such as constant pressure, constant volume or constant temperature. In this case, the Legendre transformation of the energy U is used to exchange any variable X_j with its derivative $P_j = (\partial U/\partial X_j)$. The equilibrium of the system at constant P_j corresponds to the extremum of the function $\psi = U - P_j X_j$. ψ, which is the Legendre transform of the energy U, is called the thermodynamic potential. In the present case we wish to study equilibrium at constant

temperature, by allowing perturbations of the area of contact at constant load P, or at constant displacement δ (fixed load or fixed grips conditions). Of interest are thus the Helmholtz free energy $F = U - TS$, and the Gibbs free energy $\mathcal{G} = U - TS - P\delta$, whose differentials are

$$dF = P d\delta + (G - w) dA - S dT \quad (3)$$

$$d\mathcal{G} = -\delta dP + (G - w) dA - S dT \quad (4)$$

Noting that $-P\delta$ is the potential energy U_P of the load, these expressions show that

$$G = \left(\frac{\partial U_E}{\partial A}\right)_{\delta,S} = \left(\frac{\partial U_E}{\partial A} + \frac{\partial U_P}{\partial A}\right)_{P,S} \quad (5)$$

Note that the Maxwell relations (obtained from the equality of the mixed partial derivatives of $\mathcal{G}$ or F) give

$$\left(\frac{\partial G}{\partial \delta}\right)_A = \left(\frac{\partial P}{\partial A}\right)_\delta \quad (6)$$

$$\left(\frac{\partial G}{\partial P}\right)_A = -\left(\frac{\partial \delta}{\partial A}\right)_P \quad (7)$$

with

$$\left(\frac{\partial P}{\partial A}\right)_\delta \left(\frac{\partial A}{\partial \delta}\right)_P \left(\frac{\partial \delta}{\partial P}\right)_A = -1 \quad (8)$$

Equilibrium at fixed temperature and fixed load conditions ($dT = 0, dP = 0$) corresponds to an extremum of $\mathcal{G}$, and equilibrium at fixed temperature and fixed grips ($dT = 0, d\delta = 0$) to an extremum of F. In either case equilibrium is given by

$$G = w \quad (9)$$

(The same equilibrium condition would be obtained at fixed Δ with a spring of stiffness k_m [3].) Equation 9 is the Griffith criterion which links two of the three variables δ, P, A of the equations of state (Equations 2), so that the equilibrium curves $\delta(A)$, $A(P)$, $P(\delta)$, are functions of w.

Fig. 2 represents the equation of state, Equation 2b, for a sphere of radius R, in contact with an elastic half space over an area of radius a. Superimposed on the curves $\delta(P, a)$ independent of w, are the curve $G = 0$, which is the Hertz equation for solids with zero surface energy ($w = 0$), and the curve $G = w$ which is the JKR solution [6]. Observation of equilibrium radii of contact against load or displacement give $w = 60\,\mathrm{mJ\,m^{-2}}$ for glass on polyurethane [2, 3] (varying with room humidity content).

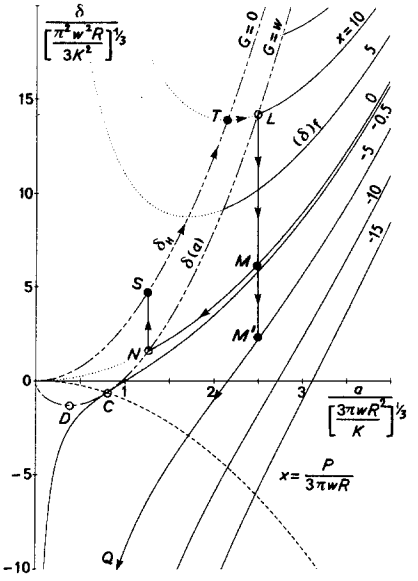

Figure 2 Relations between elastic displacement δ and radius of contact of two spheres, in reduced coordinates. The equilibrium curve is $\delta(a)$. Curves $(\delta)_P$ show the variation of δ with a at fixed load.

If $G \neq w$ the area of contact will spontaneously change so as to decrease the thermodynamic potential. If $G < w$, Equations 3 and 4 show that A must increase, and *the crack recedes*. Conversely, if $G > w$ the area of contact must decrease to give $d\mathcal{G} < 0$ or $dF < 0$, and the crack extends. $G dA$ is the mechanical energy released when the crack extends by dA. The breaking of interfacial bonds requires an amount of energy $w dA$, and the excess $(G - w) dA$ is changed in kinetic energy if there is no dissipative factor. G–w is the crack extension force, which is zero at equilibrium.

The equilibrium given by $G = w$ can be stable, unstable or neutral. A thermodynamic system under a given constraint is stable if the corresponding thermodynamic potential is minimum, i.e. if its second derivative is positive. Thus, from Equations 3 and 4 stability is defined by

$$\left(\frac{\partial G}{\partial A}\right)_\delta > 0 \text{ at fixed grips}$$

$$\left(\frac{\partial G}{\partial A}\right)_P > 0 \text{ at fixed load}$$

or more generally by $(\partial G/\partial A)_\Delta > 0$ if the

machine has a finite stiffness k_m. It can be shown that the stability range monotonically increases with the stiffness, from the fixed load case ($k_m = 0$) to the fixed grips case ($k_m = \infty$) [3, 8]. If, under a stable equilibrium, a fluctuation decreases A($dA < 0$), G incrementally decreases and one has $G < w$: the crack recedes to its equilibrium position. It can only advance if the load P or the displacement δ is slowly varied, bringing back G to the value w: one is dealing with controlled rupture of an adhesive joint*. In this case one has

$$dG = \left(\frac{\partial G}{\partial A}\right)_P dA + \left(\frac{\partial G}{\partial P}\right)_A dP = 0 \quad (10)$$

or

$$dG = \left(\frac{\partial G}{\partial A}\right)_\delta dA + \left(\frac{\partial G}{\partial \delta}\right)_A d\delta = 0 \quad (11)$$

Starting from a stable equilibrium with the two bodies compressed ($P > 0$, $\delta > 0$), let us quasistatically decrease the load: one generally encounters a progressive reduction of area of contact, i.e. a controlled rupture at $dG = 0$, until a negative load P_c is reached where $(\partial G/\partial A)_P < 0$; the equilibrium becomes unstable and the crack spontaneously extends toward complete separation at constant P_c, with $G - w$ increasing as A decreases. The load P_c corresponding to the limit of stability is the adherence force in an experiment at fixed load. At fixed grips the adherence force could be different.

For a sphere on a plane (Fig. 2), the adherence force at fixed load (Point C) is $P_c = -\frac{3}{2}\pi wR$, whereas the adherence force at fixed grips (Point D) is $P = -\frac{5}{6}\pi wR$. Quasistatic loadings or unloadings follow the equilibrium curve $\delta(a)$; but for an instantaneous unloading from P to P', i.e. an instantaneous increase in G, one observes an instantaneous displacement at constant a (Branch LM or LM') followed by a crack propagation at constant P towards a new equilibrium $G = w$ if $P' > -\frac{3}{2}\pi wR$ (Branch MN) or towards rupture if $P' < -\frac{3}{2}\pi wR$ (Branch $M'Q$). Conversely, if one applies an instantaneous loading from P' to P, G immediately decreases at constant a, but as the stress intensity factor cannot be negative, Branch ST of the Hertz curve ($G = 0$) is followed (with a tangential connection between the sphere and the half-space); the crack then *recedes* at constant load P towards its new equilibrium $G = w$ (Branch TL). Such paths have been effectively observed by Maugis and Barquins [2, 3] and the agreement with the theory is quite satisfactory.

3. Kinetics of crack propagation in viscoelastic solids

$G - w$ (or $G - 2\gamma$) is the force applied by unit length of crack. In a perfectly elastic solid, there is no dissipation and a crack subjected to a constant force $G - w > 0$ continuously accelerates. In a viscoelastic solid it undergoes a viscous drag and takes a constant speed v, a function of the temperature. The following expression has been proposed by Maugis and Barquins [2] for the kinetics of crack propagation:

$$G - w = w\phi(a_T v) \quad (12)$$

with the following assumptions:

(a) kinetic energy is neglected;

(b) the losses are limited to the crack tip zone where the stresses and the strain rates are high, so that gross displacements are elastic and G can still be evaluated by the elastic theory (with relaxed modulus) during kinetic phenomena;

(c) results at various temperatures can be shifted to a reference temperature $T_S = T_g + 50$ (where T_g is the glassy transition temperature measured at zero frequency) by using the WLF shift factor [11] a_T, where

$$\log a_T = \frac{8.86(T - T_S)}{101.6 + T - T_S}$$

so that a master curve is obtained when studying adherence as a function of the reduced parameter $a_T v$ [12–16] (a given value of $a_T v$ corresponds to either low speed at low temperature or to high speed at high temperature);

(d) viscous drag is proportional to the thermodynamic work of adhesion, as suggested by peeling experiments in various liquids [17] or on various substrates [18]. This means that losses only arise if the interface itself is capable of withstanding stress [18].

Thus, in Equation 12 surface properties (w)

*The first stable cracks that have been studied are the double cantilever beam with a wedge [9] and the Hertzian cone crack [10].

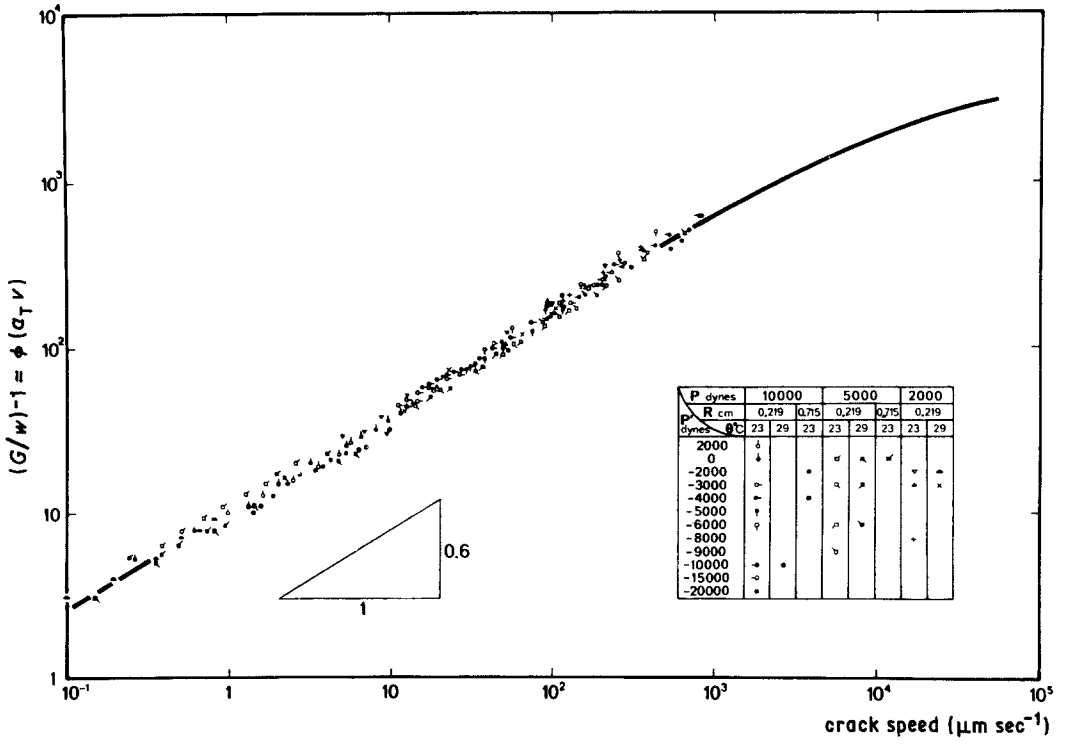

Figure 3 Reduced crack extension force against crack velocity for glass–polyurethane systems.

and viscoelastic properties (ϕ) are completely decoupled from elastic properties, geometry and loading conditions included in G. The dimensionless function $\phi(a_T v)$ is characteristic of crack propagation in Mode I in the material. Once $\phi(a_T v)$ is known, Equation 12 allows one to predict any feature such as kinetics of detachment at fixed load, fixed grips or fixed cross-head velocity.

Note that Equation 12 is different from an equation such as

$$P = P_0 f(a_T v) \tag{13}$$

where P_0 would be the quasistatic adherence force. For a sphere, for example, $P_0 = \frac{3}{2}\pi w R$ is a constant, whereas G depends on the load and the radius of contact. It is also different from a Griffith formula $\sigma \simeq (Ew/a)^{1/2}$ where w would be a rate dependent quantity.

Equation 12 was verified for glass on polyurethane for various geometries where G can be computed (sphere, flat punch, smooth-ended spheres, peeling) [2, 3, 5] by studying crack propagation at fixed load (paths such as MN or $M'Q$ for the sphere) and at various temperatures. As shown in Fig. 3, ϕ is independent of the geometry and varies as $(a_T v)^{0.6}$ over about five powers of ten, a result often found for the peeling of rubber-like materials [14, 19, 20].

Water adsorption decreases the Dupré energy of adhesion, and hence the viscoelastic losses, according to Equation 12. This point was verified by measuring the rolling resistance $\mathcal{T}$ of a glass cylinder of length l rolling on the inclined sample ($G \simeq \mathcal{T}/l$) as a function of velocity for various humidity contents [3, 20, 21]. Fig. 4 shows the translation of the $G(v)$ curves with water adsorption. As $G \gg w$ in these experiments, the shift clearly arises from the multiplicative term w on the right hand side of Equation 12. From Equation 12 the ratio of Dupré energy of adhesion w_1 in State 1 of relative humidity to that of w_2 in State 2 is given by the ratio of the strain energy release rates *at the same crack velocity*:

$$\eta = \frac{w_1}{w_2} = \frac{G_1}{G_2} \tag{14}$$

Fig. 4 gives a factor 0.5 in G between relative humidities of 30% and 70%; taking $w_1 = 50\,\text{mJ m}^{-2}$ at 70% r.h. gives $w_2 = 100\,\text{mJ m}^{-2}$ at 30% r.h. (i.e. a decrease $\Delta w = 50\,\text{mJ m}^{-2}$ by adsorption). This result is in complete agreement with

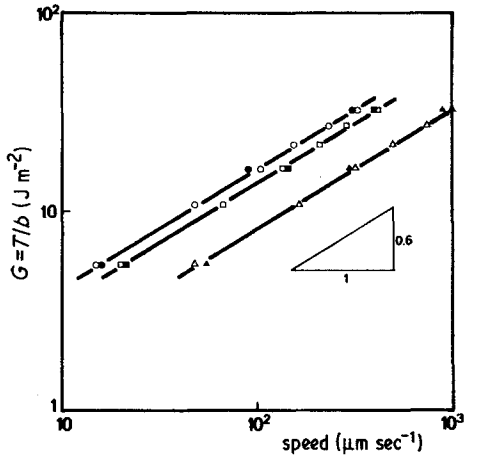

Figure 4 Rolling resistance of a glass cylinder on polyurethane for various room humidity contents: ○ 30% r.h., 760 mm Hg; ● 30%, 20 mm; □ 40%, 760 mm; ■ 40% 20 mm; △ 70% 760 mm; ▲ 70%, 20 mm.

the values deduced from the variation of equilibrium radii of contact of a glass ball on polyurethane at various room humidities. This shift in the curves is observed as long as the medium can reach the crack tip. The experiments of Carré and Schultz [22], on the peeling of elastomers on aluminium in oils of similar surface energy but of various viscosities, clearly show that one returns to the curve for peeling in air at critical velocities depending on the oil viscosity (Fig. 5).

Using the plane strain relation $G = [(1 - \nu^2)/E]K_I^2$, where ν is the Poisson ratio and E is Young's modulus for axisymmetric punches, the experimental results of Fig. 3 can be plotted as v against K (Fig. 6), and the equation

$$G - w = w\alpha(T)v^n$$

which represents the results of Fig. 3 becomes

$$v = \frac{1}{\alpha^{1/n}}\left(\frac{K^2}{K_0^2} - 1\right)^{1/n} \qquad (15)$$

where K_0 corresponds to an equilibrium crack ($G = w$). The bending of the curves, when K tends towards K_0 is very marked.

When G approaches w, the crack speed decreases and is zero for $G = w$. For $G < w$, the crack speed reverses and the area of contact increases. This point was studied by loading spheres on polyurethane [3]. As G cannot be negative, crack closure generally begins with propagation at $G = 0$; the contact is Hertzian with a tangential connection; there is no stress singularity at the crack tip ($K_I = 0$), so viscoelastic losses are negligible and crack propagation is very fast. Once the Hertzian area of contact is reached, stress singularity and discontinuity of displacement reappear, and the Mode I crack very slowly recedes to its equilibrium position with a driving force $w - G$ varying from w to 0. So, if the equilibrium radii of contact seem to be more quickly reached by loading than by unloading [23, 3], it is because most of the area of contact is instantaneously reached. Fig. 7 compares such kinetics of crack propagation and crack healing.

The adherence of solids is more often studied

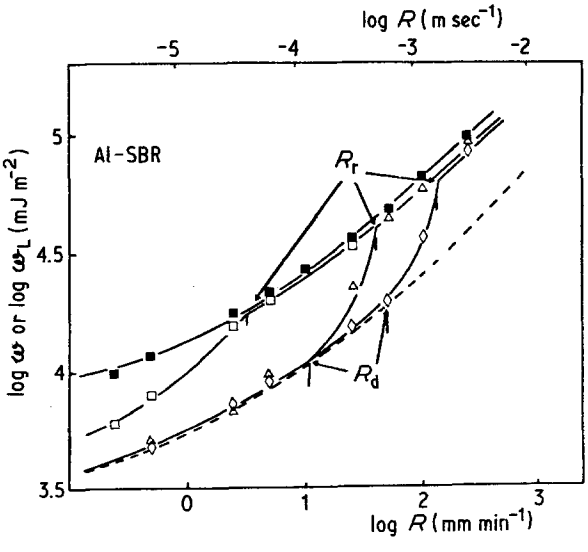

Figure 5 Peeling of elastomers on aluminium in oils of similar surface energy but of various viscosities: ■ in air; □ 12 200 cP PDMS; △ 970 cP; ◊ 340 cP (from [22]).

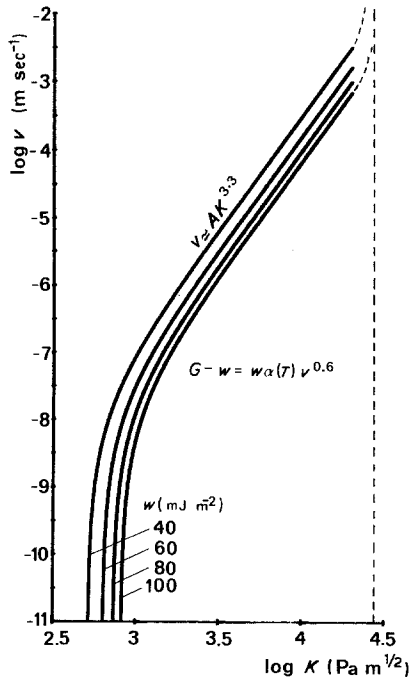

Figure 6 Results of Fig. 3 replotted in $\log v$–$\log K$ coordinates: $v = 1/2$, $E = 5 \times 10^6 \,\mathrm{N\,m^{-2}}$, $\alpha = 4.75 \times 10^4$ (20° C).

with a tensile test machine at constant cross-head velocity than at constant load, but the kinetics of separation are less easy to interpret, due to the competition for increasing G with time between increasing δ with time at constant a, and decreasing a at constant δ. If the machine has an infinite rigidity k_m (Fig. 1), one has $\dot{\Delta} = \dot{\delta}$ and the variation of G with time is given by

$$\frac{dG}{dt} = \left(\frac{\partial G}{\partial \delta}\right)_a \dot{\delta} + \left(\frac{\partial G}{\partial a}\right)_\delta \dot{a} \qquad (16)$$

The recorded force first increases, then decreases; the maximum value, termed the *tack force*, is a measure of the adherence in this particular experimental condition, and has no clear physical significance; the area under the curve, termed *tack energy*, is equal to the work $\int G da$ of the singular stress at the crack tip. "Tackiness" refers to the ability of an elastomer to adhere instantaneously to a solid surface, or to itself, after a brief time of contact under low pressure. Probe tack testing can be analysed by Equation 12, and tack curves obtained by computer integration closely coincide with experimental ones [24]. Fig. 8 is for a spherical probe and shows that even at very low cross-head velocity the viscoelastic effects considerably increase the adherence force compared to the elastic (or quasistatic) adherence force at fixed displacement (Point D).

The stability of equilibrium depends on the stiffness k_m (or the compliance C_m) of the testing machine, for elastic energy stored in the spring (Fig. 1) can be used for crack propagation. This stability is given [3] by

$$\left(\frac{\partial G}{\partial A}\right)_\Delta = \left(\frac{\partial G}{\partial A}\right)_\delta - \left(\frac{\partial P}{\partial A}\right)_\delta^2 \frac{1}{k_m + \left(\frac{\partial P}{\partial \delta}\right)_A} \qquad (17)$$

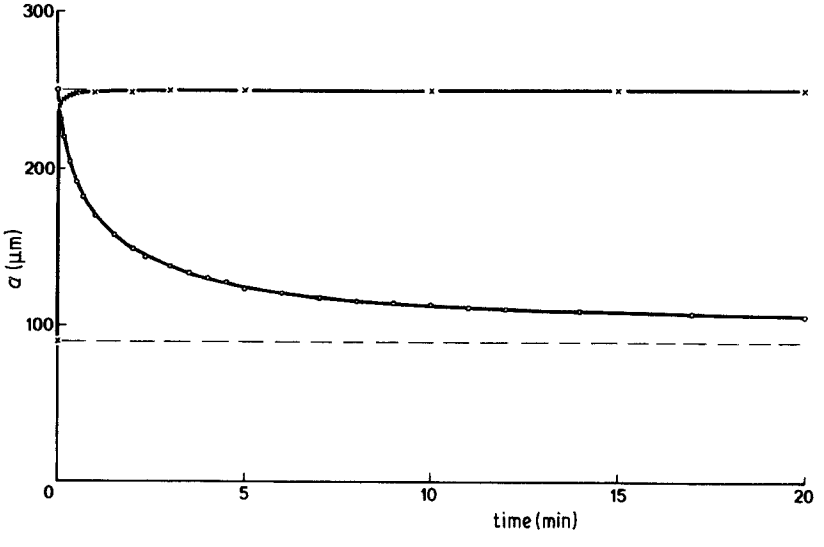

Figure 7 Radius of contact against time of a glass ball in contact with a polyurethane surface: o during unloading from $P = 50\,\mathrm{mN}$ to $P' = 0$; x during loading from $P = 0$ to $P' = 50\,\mathrm{mN}$. $R = 2.19\,\mathrm{mm}$, $E = 5\,\mathrm{MPa}$, $w = 75\,\mathrm{mJ\,m^{-2}}$. Kinetics of crack propagation and crack healing are quite different (from [3]).

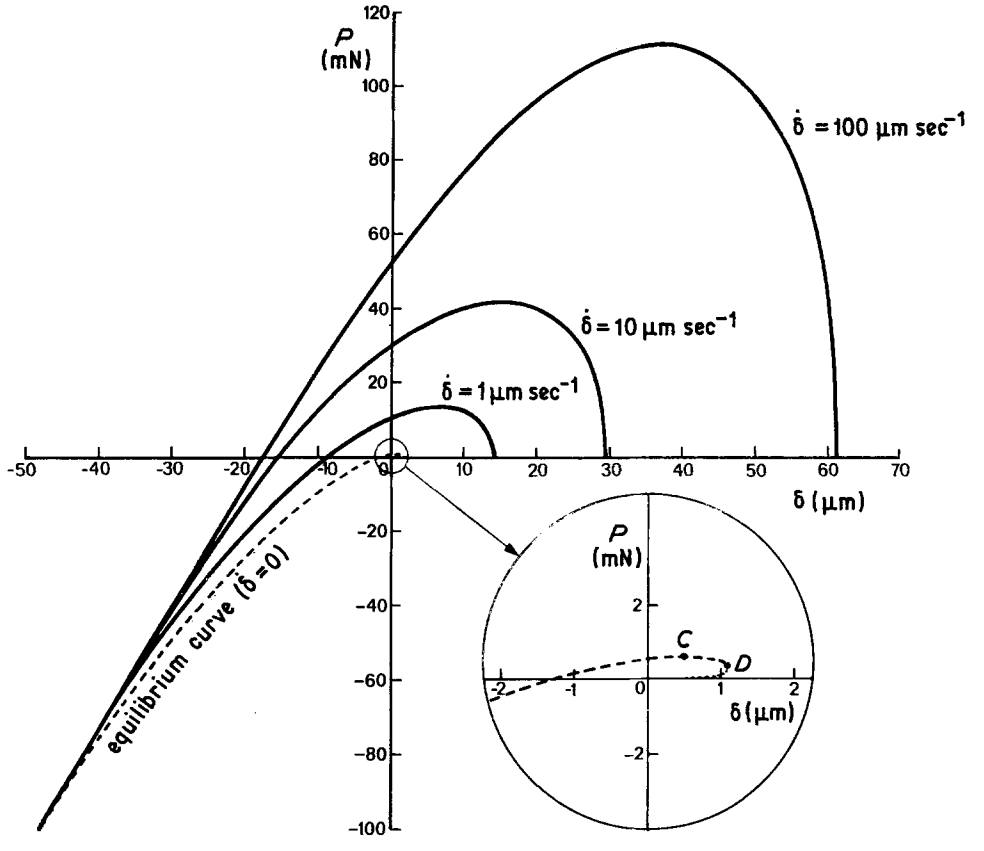

Figure 8 Glass ball on polyurethane; influence of withdrawal speed on the recorded force (tack force); $E = 3.65\,\text{MPa}$, $R = 2.19\,\text{mm}$, $w = 60\,\text{mJ m}^{-2}$, $\alpha = 4.75 \times 10^4\,\text{m kg sec A}$ (at 295 K) in Equation 15.

or in alternative form (Hutchinson and Paris [25]) by

$$\left(\frac{\partial G}{\partial A}\right)_\Delta = \left(\frac{\partial G}{\partial A}\right)_P - \left(\frac{\partial G}{\partial P}\right)_A \left(\frac{\partial \delta}{\partial A}\right)_P \times \frac{1}{C_m + \left(\frac{\partial \delta}{\partial P}\right)_A}$$

$$= \left(\frac{\partial G}{\partial A}\right)_P + \left(\frac{\partial \delta}{\partial A}\right)_P^2 \frac{1}{C_m + \left(\frac{\partial \delta}{\partial P}\right)_A}$$

where

$$\Delta = \delta + \frac{P}{k_m} = \delta + C_m P \qquad (18)$$

is the imposed cross-head displacement. The quantity $(\partial P/\partial \delta)_A$ is the stiffness of the contact (or the cracked specimen) and is positive. The fixed grips case corresponds to $k_m = \infty$, and the fixed load case to $k_m = 0$. Equation 17, which shows that $(\partial G/\partial A)_\Delta$ can be negative or zero (unstable or neutral equilibrium) whereas $(\partial G/\partial A)_\delta$ is positive, was well verified by Barquins [26] with adherence of glass balls on elastomers. Fig. 9 shows how a given displacement Δ can lead to a new equilibrium or to rupture according to the value of k_m.

As elastomers have no plastic deformation at the crack tip, the deformation is completely reversible, and they do not suffer damage from cyclic loading. Fig. 10 (from Barquins [27]) compares cyclic loading–unloading and simple unloading. The number of cycles before rupture, the life-time and the displacement can be predicted with a high accuracy using Equation 12 and assuming that crack healing is instantaneous, and that portions healed for 1 sec have low energy of adhesion (about $5\,\text{mJ m}^{-2}$) compared with the value $w = 57\,\text{mJ m}^{-2}$ after 10 min dwell time.

4. Viscoelastic losses

Viscoelastic losses at the crack tip are linked with the frequency dependence of E'', the

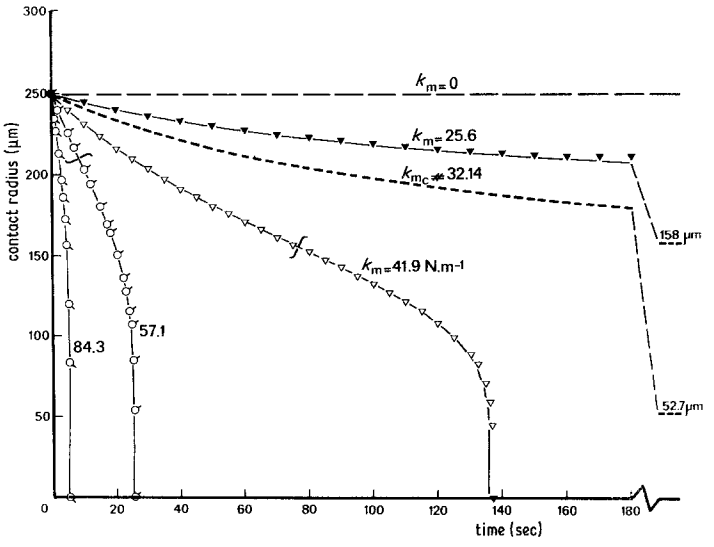

Figure 9 Variation with time of the radius of contact of a glass ball on polyurethane, for the same imposed displacement $\Delta = -1.6\,\text{mm}$ and various values of stiffness k_m (from [26]).

imaginary part of Young's modulus (loss modulus). As a matter of fact E'' varies with the frequency as $\omega^{0.6}$ for polyurethane at low frequency (Fig. 11, from [28]).

When the crack propagates and approaches a point at the interface, the stress normal to the interface rises to a maximum and then abruptly falls off to zero. In that cycle where all the frequencies ω are excited, with a frequency distribution depending on crack speed, energy is lost, and the problem is to connect the frequency dependent $E'(\omega)$ and $E''(\omega)$ to the speed dependent $\phi(v)$. Since the elastic solution for crack propagation is known, the theory of viscoelasticity allows us in principle to deduce the viscoelastic strain energy release rate $G_{\text{visc.}}$ from a knowledge of $E'(\omega)$ and $E''(\omega)$. A number of tentative attempts have recently been made [29–33] and Christensen (private communication) has pointed out that Equation 12 directly follows from his general theory [30] and did not need to be assumed. One can hope that in the near future, the function $\phi(a_T v)$ will be directly derived from measurements of $E'(\omega)$ and $E''(\omega)$.

Note that a viscoelastic model such as the parabolic Zener model

$$E^*(i\omega) = E_0 + \frac{E_\infty - E_0}{1 + (i\omega\tau)^{-n}}$$

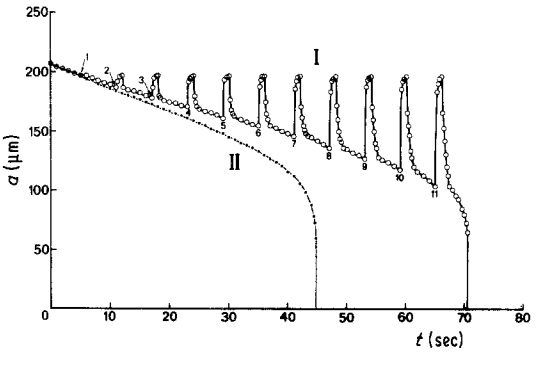

Figure 10 Variation with time of the contact radius of a glass ball on polyurethane for rectangular cyclic loading from $P = 30\,\text{mN}$ ($t_A = 1\,\text{sec}$) to $P' = -30\,\text{mN}$ ($T_R = 5\,\text{sec}$). Eleven cycles are observed before rupture. Curve II shows the evolution of the contact radius for a simple unloading from P to P' (from [27]).

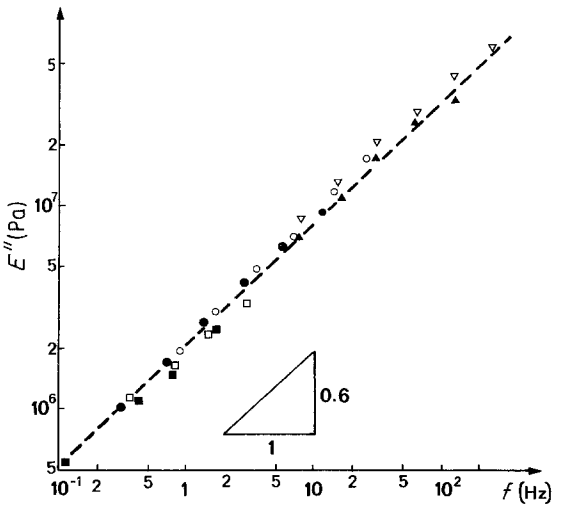

Figure 11 Master curve for loss modulus in polyurethane: ▽ 20° C; ▲ 22° C; ○ 30° C; ● 36° C; □ 40° C; ■ 50° C (from [28]).

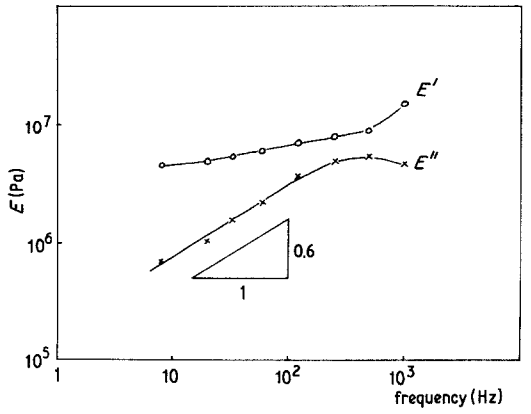

Figure 12 Frequency dependence of E' and E'' for polyurethane (from [7]).

must be used to have $E''(\omega) \simeq (\omega\tau)^n$ when $\omega\tau \to 0$. Such a model corresponds to a continuous spectrum of relaxation times, and leads to a symmetrical Cole–Cole diagram with $E''(\omega) \simeq (\omega\tau)^{-n}$ when $\omega\tau \to \infty$.

At sufficiently high frequencies or low temperatures, the loss modulus decreases (Fig. 12), and the behaviour tends to become elastic, so $\phi(a_T v)$ would decrease with v at higher speed. A number of observations on peeling [12, 34] or rolling [20] confirm this point. The implication of such a negative-resistance branch is discussed below.

5. Negative resistance

A simple argument shows that a negative-resistance branch cannot be observed: if the crack accelerates, the resistance to crack propagation decreases, and the crack further accelerates, and conversely if the crack slows down, so that stable crack propagation cannot occur. This can also be proved by a more sophisticated thermodynamic argument.

Comparing Equation 1 with the principle of energy conservation

$$\mathrm{d}U + \mathrm{d}K = P\mathrm{d}\delta + \mathrm{d}Q \qquad (19)$$

where $\mathrm{d}Q$ is the heat received, and neglecting the variation $\mathrm{d}K$ of kinetic energy, it becomes

$$T\mathrm{d}S = \mathrm{d}Q - (G - w)\mathrm{d}A \qquad (20)$$

Comparing with

$$T\mathrm{d}S = \mathrm{d}Q + T\mathrm{d}_i S$$

it appears that the entropy produced in the system is

$$\mathrm{d}_i S = -\frac{1}{T}(G - w)\mathrm{d}A \qquad (21)$$

Crack propagation at $G = w$, like the branch LN in Fig. 2, is thus a reversible process. The entropy production rate (a non-negative quantity) is

$$P[S] = \frac{\mathrm{d}_i S}{\mathrm{d}t} = -\frac{1}{T}(G - w)\frac{\mathrm{d}A}{\mathrm{d}t} \geqslant 0 \qquad (22)$$

as pointed out by Rice [35]. Letting

$$X_k = \frac{G - w}{T} = \frac{w\phi(v)}{T}$$

and

$$J_k = -\frac{\mathrm{d}A}{\mathrm{d}t} = 2\pi a v$$

the generalized force and flux, the condition of stability of this irreversible process of energy dissipation (Glansdorff and Prigogine [36]) corresponds to a non-negative value of the excess entropy production rate:

$$\sum_k \delta J_k \delta X_k \geqslant 0 \qquad (23)$$

i.e.

$$\frac{2\pi a w}{T}\delta\phi\delta v \geqslant 0$$

where δ refers here to small increments. The condition of stable crack propagation is thus

$$\frac{\mathrm{d}\phi}{\mathrm{d}v} \geqslant 0 \qquad (24)$$

The negative-resistance branch of $\phi(v)$ cannot be observed. This condition of stable or unstable crack propagation (a material property) must not be confused with the condition of stable or unstable equilibrium defined by the sign of $\partial G/\partial A$, which is a property of the tested geometry.

However, the resistance to crack advance cannot continuously decrease. Other positive branches due to a complicated loss spectrum can occur, but anyway the crack speed cannot exceed the Rayleigh velocity C_R, and G (deduced from external forces by formulae valid for quasistatic cracks) increases toward infinity as $v \to C_R$, so that the curve log G–log v can be seen as the superposition of a curve for brittle fracture with dynamic effects, and a curve for viscoelastic losses (Fig. 13). Let G_c be the critical

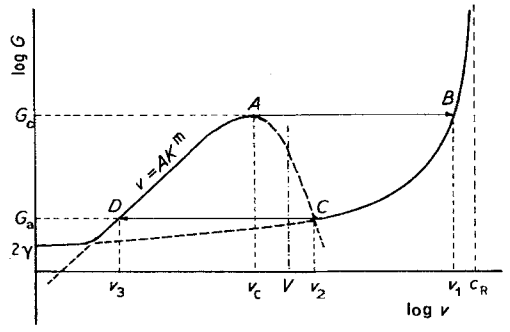

Figure 13 Schematic diagram of a log G–log v curve showing viscoelastic effects.

strain energy release rate corresponding to the end of the first positive branch, at a speed v_c such that

$$G_c = w\,[1 + \phi(v_c)] = w_f \qquad (25)$$

The crack takes a constant velocity v at constant G as long as $G < G_c$ (subcritical crack growth). At G_c the crack velocity jumps on a second-position branch, and rupture appears catastrophic. In this model one has:

$G < w$ (or 2γ) crack closure

$G > w$ (or 2γ) crack advance

w (or 2γ) $< G < G_c$ subcritical crack growth

$G \geqslant G_c$ catastrophic crack propagation.

If v_c is small, the subcritical crack growth is not apparent and the condition $G = G_c$ for crack velocity discontinuity and catastrophic failure can easily be confused with the Griffith condition $G = 2\gamma$ (or w) for crack equilibrium by writing $G = 2\gamma_f$ (or w_f) where γ_f is a "fracture surface energy". (For glass–polyurethane G_c is a thousand times the Dupré energy of adhesion.) However, if so, subcritical crack growth in a vacuum becomes incomprehensible, and stress corrosion must be invoked to explain the increase in crack velocity in the presence of an environment. As we will see below this proposed model can also explain embrittlement effects and stick–slip crack motion when a mean velocity is imposed in the negative-branch range.

6. Subcritical crack growth in glasses and ceramics

Delayed failure in glasses has been known since the early work of Grenet [37] and Milligan [38]. The existence of a threshold stress approxi-

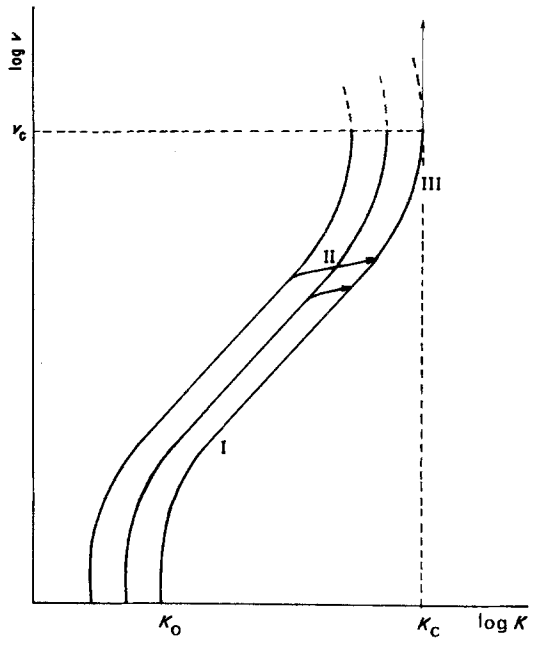

Figure 14 Schematic diagram for subcritical crack growth in glass.

mately 20 to 30 % of the short-time failure stress was shown by Holland and Turner [39]. That phenomenon of delayed failure was termed static fatigue by Baker and Preston [40] who emphasized the influence of humidity. The first measurements of crack velocity in water vapour were performed by Wiederhorn [41, 42] using double cantilever beam (DCB) specimens. Crack velocities were first reported as a function of applied load [41, 42], and later plotted against stress intensity factors [43, 44] (eliminating crack length and specimen geometry), and the three regions I, II, III of the curves (Fig. 14) were described, with Region II claimed as corresponding to crack motion limited by the rate of transport of water to the crack tip. Evans [45] introduced the double torsion (DT) test, more suitable for studying very slow crack propagation, and following Charles [46] showed that the empirical equation

$$v = A(T)K^m \qquad (26)$$

can fit most of the v, K curves in Region I and can be used for lifetime predictions. Although the presence of water is of first importance, subcritical crack growth has been observed in a vacuum [47, 48].

A number of theories have been proposed to explain subcritical crack growth and have been

reviewed [49]. In the model proposed here by analogy with the results for adherence of viscoelastic solids, the static fatigue limit K_0 of glasses and ceramics corresponds to an equilibrium crack and gives the intrinsic surface energy. When $K > K_0$ the crack advances according to the Griffith criterion, with a velocity v depending on the loss spectrum (internal friction) of the material, and the phenomenological equation

$$G - 2\gamma = 2\gamma\alpha(T)\phi(v) \qquad (27)$$

can be used. For temperatures below T_g the WLF shift factor (Equation 13) cannot be used and the temperature dependence is described by an unknown function $\alpha(T)$. As noted by Wiederhorn *et al.* [48] and Freiman [50], the critical stress intensity factor is simply one point on the v–K curve where the velocity sharply increases. It is assumed here that at K_c the crack velocity jumps to higher values. In Region I on a wide range of crack velocities, the function $\phi(v)$ has the form $\phi(v) = v^n$ and Equation 27 becomes

$$v = \frac{1}{\alpha^{1/n}}\left(\frac{K^2}{K_0^2} - 1\right)^{1/n} \qquad (28)$$

which gives Equation 26 with $m = 2/n$ for $K \gg K_0$. This equation takes into account the bending of v–K curves near K_0, clearly visible below $10^{-9}\,\mathrm{m\,sec^{-1}}$ in published results [44, 45, 51–54], and allows for a more precise lifetime prediction. Unfortunately no clear value of K_0 in a vacuum can be found. In the presence of humidity the whole $\log v$–$\log K$ curve is shifted towards lower values of K (Fig. 14), but this phenomenon is obscured by the limitation of the arrival rate of vapour or viscous drag of water at the crack tip (Region II) and one generally returns (sometimes after cavitation, see Section 7) to the vacuum values (Region III) at high velocity. In the presence of humidity the static fatigue limit K_0 can be reduced* to $K_0 = 0.37\,\mathrm{MPa\,m^{1/2}}$, i.e for plane stress (with DCB, compact tension (CT) or DT specimens) a surface energy $\gamma = 0.9\,\mathrm{J\,m^{-2}}$ for silica [56], $K_0 = 0.25\,\mathrm{MPa\,m^{1/2}}$ ($\gamma = 0.45\,\mathrm{J\,m^{-2}}$) for soda lime [44, 52] or borosilicate in water [44], whereas the critical stress intensity factors are $K_c = 0.80\,\mathrm{MPa\,m^{1/2}}$, i.e. $\gamma_f = 4.4\,\mathrm{J\,m^{-2}}$ for silica [56, 57] and $K_c = 0.76\,\mathrm{MPa\,m^{1/2}}$ i.e. $\gamma_f = 3.9\,\mathrm{J\,m^{-2}}$ for soda lime [48, 57]. The ratio γ_f/γ is thus relatively small for glass (about 10) compared to that for elastomers (about 1000).

As in Section 3, the ratio of the surface energy γ_1 in Environment 1 to that γ_2 in Environment 2 is given from Equation 27 by the ratio of strain energy release rates *at the same crack velocity* and temperature (not at the same cross-head speed):

$$\eta = \frac{\gamma_1}{\gamma_2} = \frac{G_1}{G_2} = \frac{K_1^2}{K_2^2} \qquad (29)$$

Estimates from the literature data give the ratio 0.6 for soda lime between 0.017% and 100% r.h. [52], 0.5 for commercial glass between octanol with 15% humidity and water [58], 0.6 for soda lime in butyl alcohol solutions with different quantities of dissolved water [59], 0.7 for silica glass between 0.08% r.h. and water [56]. Taking the surface energy in 100% humidity as $\gamma_1 = 0.45\,\mathrm{J\,m^{-2}}$ for glass and $\gamma_1 = 0.9\,\mathrm{J\,m^{-2}}$ for silica, the variation of surface energy $\Delta\gamma$ by water adsorption are respectively 0.30, 0.45, 0.30 and $0.40\,\mathrm{J\,m^{-2}}$. These reductions in surface energy must be in agreement with the Gibbs adsorption formula

$$\Delta\gamma = -RT\int_0^{p_{sat}} \Gamma\,\frac{dp}{p} \qquad (30)$$

where Γ is the adsorption in moles per unit area at the pressure p. Such determination of $\Delta\gamma$ on quartz powder by Boyd and Livingston [60] or glass powder by Schultz and Simon [61] gave respectively $\Delta\gamma = 0.25$ and $0.23\,\mathrm{J\,m^{-2}}$ in saturated water vapour, which is of similar order of magnitude. The intrinsic surface energy of glass in a vacuum can thus be estimated to be about $0.8\,\mathrm{J\,m^{-2}}$.

Similar shifts of $\log v$–$\log K$ curves with water adsorption have been observed on PMMA [62] and epoxy resins [63] with a ratio G_1/G_2 of about 0.5.

Note that the idea of K_0 corresponding to intrinsic surface energy has been already proposed by Hasselman *et al.* [64] and Rice [35]. Orowan [65] proposed that the reduction of failure stress in long-term experiments could be explained by a reduction by a factor of ten in surface energy from the value γ_f in vacuum to the value γ in moist air. This is a typical confusion

*At these low K values, great care must be taken to avoid residual stresses. In particular the groove cut along CT, DT or DCB specimens to guide the crack, can introduce errors, if not properly annealed [55].

between G_c and the Griffith criterion. Michalske and Freiman [66] recently proposed a molecular interpretation of stress corrosion in silica, suggesting that environments which enhance stress corrosion are composed of molecular groups with electron donor sites on one end and proton donor sites at the other. This is not in contradiction with reduction of surface energy by adsorption, and reflects the quantum mechanical aspect of modern theories of adsorption. Weidman and Holloway [51] in their experiments on DT specimens of glass observed that the change in crack speed following a change in load was instantaneous and that the same crack speed was obtained at any given load, irrespective of whether the previous load was larger or smaller than the given one. This is very similar to the results of Maugis and Barquins [2] on adherence of elastomers. Note also how the transition Region II closely resembles the transition observed by peeling elastomers in liquids of various viscosities [22].

For $K < K_0$ the crack must heal according to the Griffith criterion. Such crack healing in brittle solids has been studied in a number of papers, as reported by Hockey [67]. Wiederhorn and Townsend [68] have shown that recovery of strength during healing was approximately 80% for cracks formed by shock. Observations of brittle crystalline solids in the transmission electron microscope [67, 69, 70] have revealed interfacial misfit dislocations which form when crack interfaces rebond in imperfect registry, and no evidence for crack tip plasticity. It is this absence of plasticity which explains why the static fatigue limit of glasses and ceramics corresponds to equilibrium cracks and to the true Griffith criterion. It explains also that glasses and ceramics, unlike metals, do not suffer damage from cyclic loading and that crack growth rates obtained under cyclic stress conditions can be directly predicted from slow growth studies [71–74] as observed on cyclic fatigue at glass–elastomer contact by Barquins [27].

The surrounding medium can have two opposite effects. It generally reduces the surface energy and thus the strength of the material, but if not saturated with the components of the material it can dissolve surface layers, including surface cracks, and blunt the crack tips, thus increasing the strength. This Joffe effect, well studied by Stokes *et al.* [75], can be exemplified with an irradiated KCl crystal [76]: such a crystal is weak and brittle if deformed in air, but up to 25 times stronger and considerably more ductile if deformed in water, i.e. while being slowly dissolved. Glass left in air or immersed in water or acid in the absence of stress (ageing) tends to gain strength [77–82]. So, water strengthens glass at stresses below that of the static fatigue limit and weakens it at stresses greater than that of the static fatigue limit [41]. Another complication with corrosive media is the ion exchange between surface layers and the solution causing internal stresses and spontaneous cracking [83, 84].

Fracture surface energies of glass and ceramics have sometimes been evaluated by the work of fracture [85–88] by measuring the area below the load–displacement curve. This work of fracture is quite similar to the tack energy of elastomers [24]. Its value $\int_{A_0}^{0} G \mathrm{d}A$ is not a material property (except for quasistatic crack propagtion at $G = 2\gamma$); it depends on the crosshead velocity (Fig. 8) and on the stiffness of the apparatus.

7. Velocity jump, stick–slip and acoustic emission

Let us return to Fig. 13. It was said, in Section 5, that as long as $G < G_c$, subcritical crack growth is observed with $v < v_c$. When $G = G_c$, the velocity jumps to v_1, on the second positive branch. On the other hand, if a mean velocity V is imposed, unstable crack growth will be observed. The velocity jumps from A to B at G_c, but this velocity is too high and the crack slows down to Point C where the velocity is still too high, then jumps to Point D where the crack seems arrested; the velocity increases to v_c (too low) and jumps to Point B. A stick–slip motion thus occurs, where most of the time is spent on the slow crack growth branch DA.

7.1. Velocity jump or stick–slip?

Whether velocity jump or stick–slip motion occurs depends on the stability of the system given by Equation 17. This stability depends not only on the geometry of the specimen, but on the loading system [a classical example is DCB (see Appendix) where $(\partial G/\partial A)_p < 0$ and $(\partial G/\partial A)_\delta > 0$]. If $(\delta G/\partial A)_\Delta < 0$, G continuously increases as the ligament A decreases, the velocity cannot be controlled and velocity jump occurs. If

$(\partial G/\partial A)_\Delta > 0$, the rupture is controlled, the crack velocity v is a function of the crosshead velocity $\dot{\Delta}$, and stick–slip occurs if one tries to impose a mean velocity between v_c and v_2. The first case corresponded to DCB at fixed load or single edge notched (SEN) specimens tested with an Instron machine. The second case corresponds to DCB, tapered DCB (TDCB), DT specimens and peeling. (The three last geometries have a neutral equilibrium.) Velocity jump and stick–slip are easily observed in polymethyl methacrylate (PMMA) and epoxy resins where v_c is relatively low.

7.2. Velocity jump

Velocity jump in PMMA has been observed by Berry [89], Marshall *et al.* [90], Döll and Weidmann [91], Margolis *et al.* [92] with SEN specimens, and by Dobbs *et al.* [93] on tension specimens with an internal "penny-shaped" crack produced by a laser. At room temperature the velocity jumps from about 0.1 to about 10 to 100 m sec^{-1}. This jump, associated with acoustic emission, occurs at K_c and is always preceded by slow crack growth. Fig. 15 (from [92]) shows P–δ curves at $\dot{\Delta} = 5\,\text{mm min}^{-1}$ for SEN specimens with various initial crack lengths. Slow crack propagation commences *on the straight line* and then deviates until a load P_{max} is reached. Slow crack growth still operates beyond P_{max}, and the slow to fast transition occurs approximately at Point S. Clearly P_{max} is the exact analogue of tack force in Fig. 8 (computed from the law for subcritical crack growth) and has no simple physical significance. Its value depends on the cross-head velocity $\dot{\Delta}$. Since K_c at instability is generally computed from P_{max} and the crack length taken as the initial length plus the slow crack growth portion measured on the fracture surface, its value can be in error. Determination of K_c would be more accurate with experiments at fixed load, although experiments by Marshall *et al.* [90] show that K_c is not sensitive to $\dot{\Delta}$ above $-50°$ C.

7.3. Stick–slip of the first kind

Stick–slip is a widely observed phenomenon. The first published results are probably those of Bailey [94] on cleavage of mica, Dannenberg [95] on blister tests in adherence, Gardon [34], and Broutman and McGarry [96] on DCB specimens of PMMA. Stick–slip is more easily studied by

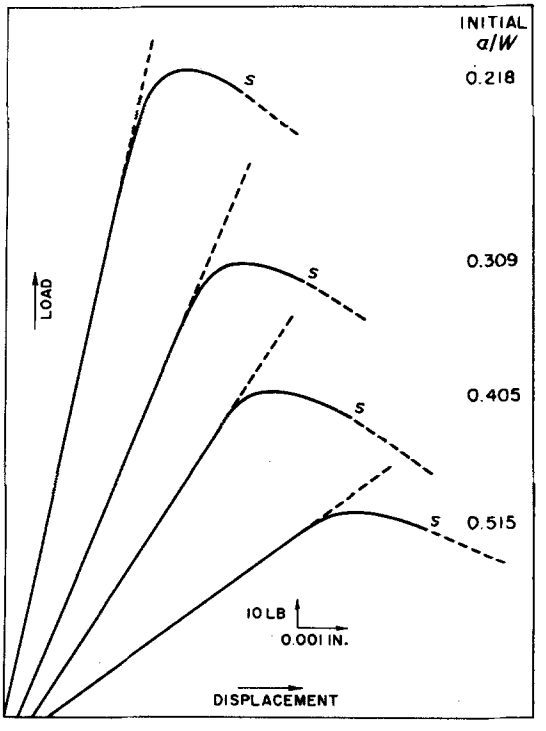

Figure 15 Load displacement (P–δ) curves for PMMA SEN specimens with various initial crack lengths. Cross head velocity $\dot{\Delta} = 5\,\text{mm min}^{-1}$ (from [92]).

peeling, for G is proportional to the applied load and independent of crack length [97, 98]:

$$G = \frac{P}{b}(1 - \cos\theta) \qquad (31)$$

Take an adhesive tape and pull it. At low velocity the motion is continuous and the crack velocity v is related to pull rate $\dot{\Delta}$ by

$$v = \dot{\Delta} - \frac{d\delta}{dt}$$

where δ is the elastic elongation (Hooke's law). At higher speed it is jerky with characteristic acoustic emission, and the wavelength of transverse striations increases linearly with the peeled length L [99] (due to variation of stiffness with length); at very high speed it becomes continuous again. Place it in a refrigerator for a moment; the motion is jerky at very low speed. Heat it at about 40° C, and the motion is continuous. This temperature dependence is accounted for by the WLF shift factor a_T (Equation 13). Fig. 16 (from [100]) is such a master curve for pulling rates between 5×10^{-3} and 10^2 cm min^{-1}, and temperature between 312

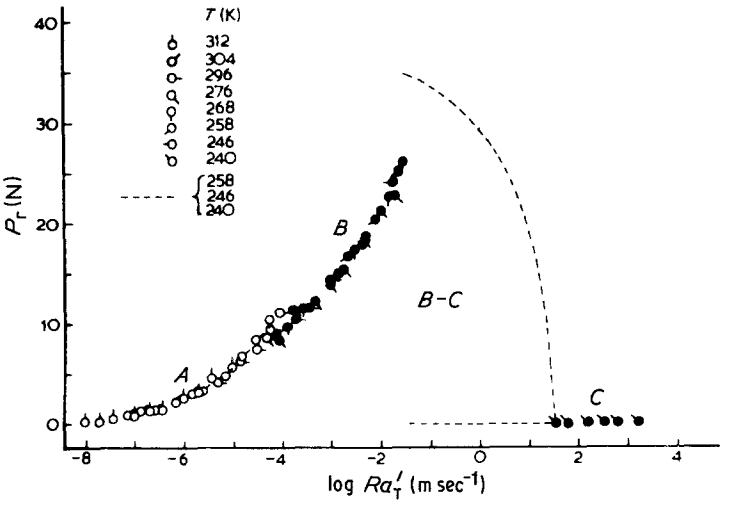

Figure 16 Master curve of peel force against pulling rate at 296 K for the system 6:4 NR/Piccolyte S115: ○ cohesive separation; ● adhesive separation (from [100]).

and 240 K. Regions *A*, *B* and *C* are the stable branches, and stick–slip occurs in region *BC* with an amplitude decreasing with pulling rate. Sometimes three stable branches and two stick–slip regions can be observed [14]. However, as stick–slip in adhesive systems can be obscured by the adhesive–cohesive transition, we will examine stick–slip in PMMA and epoxy resins.

Stick–slip in glassy polymers has been studied with DCB, TDCB, DT and CT specimens. In epoxy resins, it occurs even in a vacuum [101] and is thus an inherent property of materials. When only one stable branch can be observed, unstable crack propagation can be obtained either by lowering the cross-head velocity as in most epoxy resins, or by increasing it as in PMMA. For epoxy resins at room temperature in air, Young and Beaumont [102] have shown that continuous propagation is not possible below a crack velocity of 6×10^{-4} m sec^{-1}. This velocity can thus be considered as the velocity v_2 of Fig. 13. For PMMA, as shown by Marshall *et al.* [90], the limit of stable velocity K_c, v_c (Point *A* in Fig. 13) below which crack velocity is given by Equation 26 corresponds to the point of velocity jump observed with SEN specimens. P–δ curves during stick–slip have a characteristic "sawtooth" aspect with two discontinuities, the higher giving K_i, G_i at crack initiation, the lower giving K_a, G_a at crack arrest. From Fig. 13, it would be anticipated that K_i and K_a remain constant and equal to the maximum and the minimum of the curve, when the mean velocity V varies from v_c to v_2. However, the experimental results on stick–slip show that K_i decreases and K_a slightly increases with the mean velocity V, as shown in Fig. 17 (from [103]) and in Fig. 16.

This probably arises from inertial effects which have been neglected in the model. When the difference between K_i and K_a is large, propagation occurs by large jumps, whereas when it is small the jumps are small, and when K_i is equal to K_a, the propagation is continuous [103]. Slowing down of the crack (from *B* to *C*) has been reported by Yamini and Young [103], and the smooth decrease of G from G_i to G_a by Mostovoy *et al.* [104]. As discussed above, the

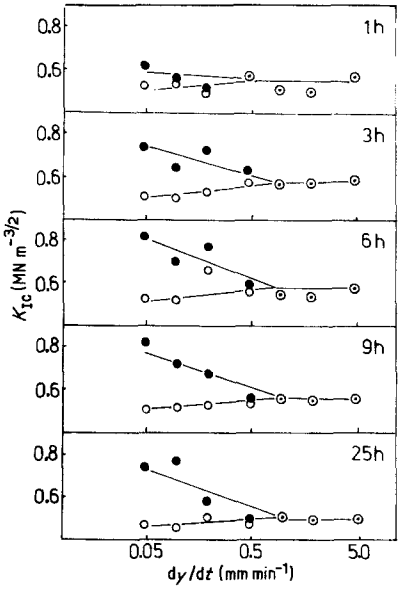

Figure 17 Variation of K_{ICi} and K_{ICa} with cross-head speed on Epikote 828 specimens for different curing periods (from [103]).

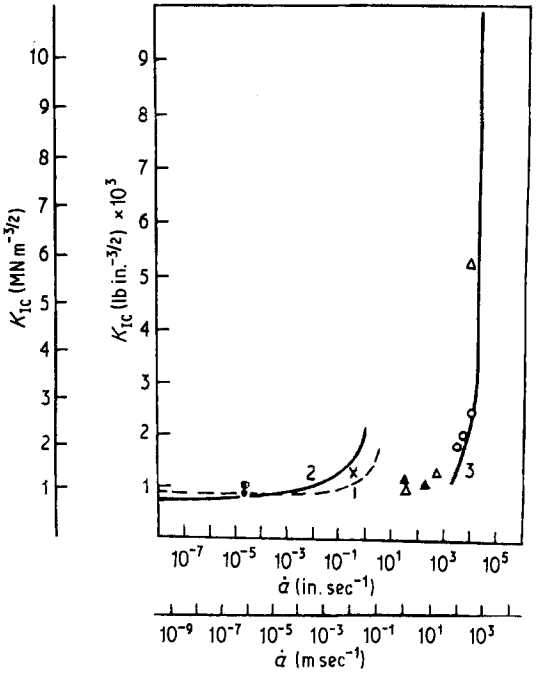

Figure 18 Dependence of crack velocity on driving force for PMMA (from [107]; symbols refer to sources quoted therein).

stability depends on the stiffness of the testing machine. When the stiffness is decreased, for example, by inserting a plastic wedge instead of an aluminium wedge in a DCB [105] or by inserting a soft spring between the machine and a peeled tape [106], the stick–slip wavelength increases. At the limit $k_m \rightarrow 0$ one has an infinite wavelength corresponding to the velocity-jump case at fixed load.

Fast propagation along the second positive branch in PMMA has been studied by Green and Pratt [107] who showed that, contrary to what is observed at low crack velocity, the stress intensity factor must be increased five- to ten-fold for increase of the crack velocity by one order (Fig. 18). Similar results have been obtained by Mostovoy *et al.* [104] for epoxy adhesives. Note that Broutman and Kobayashi [108] have described a second discontinuity at approximately 50 m sec^{-1} in PMMA in addition to the one at 10^{-1} m sec^{-1}. At these high G values on the second stable branch, G can reach G_c ahead of the crack tip, especially at stress concentrators such as inclusions, so that fast cracks can be created ahead of the main crack. These secondary fractures extending radially interfere with the primary crack to give parabolic or hyperbolic markings, as first observed by Kies *et al.* [109] on polymers and Smekal [110] on glass, and further studied by Cotterell [111]. The author has attempted to rationalize the smooth and rough fracture surface, or the "mirror" and "mist", with the various regimes of crack propagation, but the situation is not clear.

Velocity instabilities were early associated with decreases in crack resistance, with velocity leading to auto-accelerating effects [8, 12] expressed as $dG/dv < 0$ or $dR/dv < 0$. Various reasons have been invoked for this decrease: molecular relaxation and internal friction [112], isothermal to adiabatic transition causing thermal softening [113], and transition in craze formation [107]. The very sensitive influence of curing agents, the low velocity at which stick–slip can be observed, and the absence of craze in epoxy resins give more probability to internal friction effects. Curves with a negative branch between two positive ones have been published [90, 113]. A cycle similar to that proposed here was given by Aubrey *et al.* [114] to explain stick–slip in peeling, but the second positive branch and the portion *BCD* of the cycle were not described.

7.4. Velocity jump and stick–slip associated with cavitation

A second kind of stick–slip exists, first observed by Benbow [115] in PMMA. If a slow, stable crack is wetted with water, the crack apparently stops growing and the clamped ends of the specimen can be separated by a considerable amount before the crack jumps forward. When the crack jumps forward it is travelling in dry material and reaches the position it would have had in the absence of water (Fig. 19). The apparent fracture energy can be raised to four times that of the dry material by the addition of water. Similar results with DT specimens were found by Hakeem and Phillips [116, 117] with methanol, and Mai [118] with CCl_4. In epoxy resins where stick–slip is observed at low speed and continuous propagation at high speed, the effect of water can be to suppress continuous propagation and cause the crack to jump over the entire range of cross-head displacement rates used, as observed by Yamini and Young [101, 103], or to change propagation from unstable to stable [119].

Explanations can be found from the beautiful

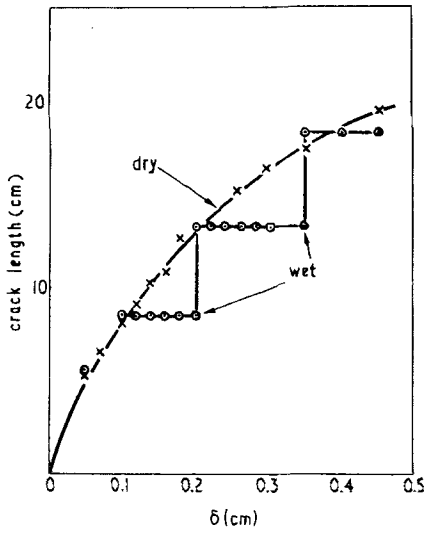

Figure 19 Influence of wetting on crack propagation in PMMA (from [115]).

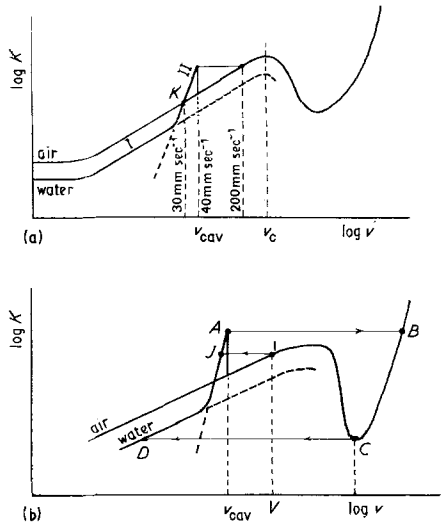

Figure 20 Schematic diagrams showing the effect of viscous drag at the crack tip.

experiments of Frechette and co-workers [120–122] on the propagation of cracks partially filled with water in SEN specimens of glass. For crack velocities below 30 mm sec^{-1}, water facilitates crack propagation compared to air, as discussed in Section 6; at about 30 mm sec^{-1} (equivelocity point, Point K) wetted and non-wetted cracks require the same stress intensity factor, whereas at velocities above 30 mm sec^{-1} the viscosity hinders crack propagation until cavitation occurs at v_{cv} = 40 mm sec^{-1} and crack velocity instantaneously jumps to its values on the dry curve (Fig. 20a). A scarp is formed on the fracture surface at the point where the velocity jumps from 40 to 200 mm sec^{-1}, and the appearance of fine cavitation bubbles at velocities slightly lower than v_{cv} explains the formation of hackles. A slight modification of Fig. 20a can account for stick–slip in PMMA in the presence of liquids. Let us assume that K for cavitation is higher than K_c in air (Fig. 20b). An imposed velocity V gives stable propagation in air (Point I). Inserting a liquid causes an apparent crack arrest (Point J), so that displacement and stress intensity factor must be increased until cavitation occurs at Point A. The velocity jumps to Point B, and a stick–slip cycle $ABCD$ occurs at the mean velocity V. If V is lowered below v_{cv} stick–slip disappears. If the velocity for cavitation is higher than v_c, stick–slip propagation in air can be changed into stable propagation in liquid for $v_c < V < v_{cv}$. These interpretations are speculative and need further experiments for confirmation.

In Branch II of Fig. 20a the resistance to crack advance comes essentially from viscous drag in the liquid, and energy losses at the crack tip within the material becomes negligible. The situation is thus quite similar to that described in the very elegant paper by Burns and Lawn [123]. They inserted a wetting liquid between two glass strips and ruptured the film by driving in a wedge, as in DCB experiments at fixed grips. The stable equilibrium was correctly given by $G = 2\gamma$, where G is the strain energy release rate for DCB, computed from the glass arms only and γ the surface energy of the liquid. They noted the influence of viscosity: for water, periods of several minutes were required to reach equilibrium, and for heavy oils, viscosity prevented equilibrium from being reached within a period of days. In such a case, the crack velocity v would be proportional to the driving force $G - 2\gamma$ (Newtonian viscosity) and for $G \gg 2\gamma$, log G–log v and log K–log v would display slopes of 1 and $\frac{1}{2}$ respectively. Fig. 5 clearly shows this slope in the transition zone at the two lower viscosities, and Fig. 21 (from Williams and Marshall [124]) for glass in paraffin shows both the slope of $\frac{1}{2}$* and the velocity jump studied by Michalske and Frechette [122].

Hydrodynamic phenomena and conditions

*The same slope in Region II can be found in [125].

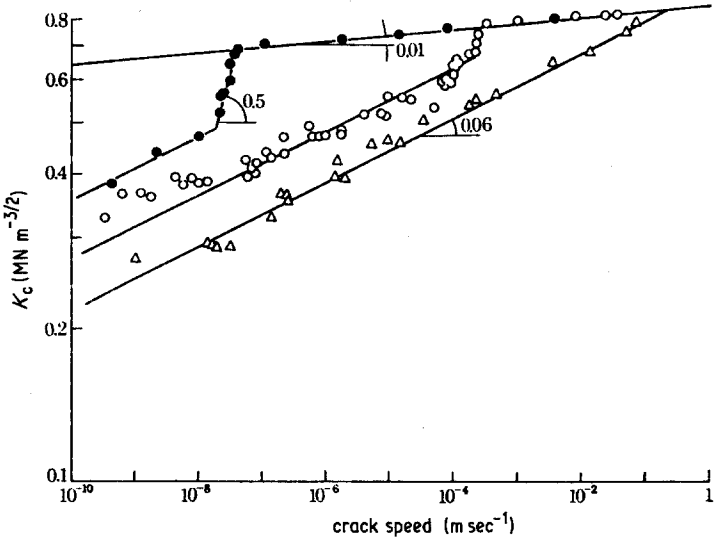

Figure 21 Crack growth rate for inorganic glass in various environments: △ water; ○ air (50% r.h.); ● dry paraffin (from [124]).

for cavitation in cracks filled with liquids have been discussed by Perrone and Liebowitz [126], Newman and Smyrl [127], Wiederhorn [49], Carré and Schultz [22] and Michalske and Frechette [122]. These last authors proposed the following equation for cavitation velocity:

$$v_{cv} = \frac{\left(\frac{2\gamma_L}{r} + P\right)\alpha^2}{2\mu(X_2^{-1} - X_1^{-1})} \qquad (32)$$

where γ_L and μ are surface energy and viscosity of the liquid, r the radius of the bubble which just fits in the crack opening, P the external pressure, α the half-angle crack opening, and X_1 and X_2 are the positions of the open end of the crack and the cavitation bubble respectively.

7.5. Acoustic emission

In the proposed model, acoustic emission occurs only when the crack velocity jumps from one positive branch to the other, in agreement with Rose's [128] proposal that acoustic emission corresponds to a crack starting or stopping abruptly. This is in apparent contradiction with the results of Evans and Linzer [129], Evans *et al.* [130] and Nadeau [131] showing that the rate of acoustic emission in glass exhibits the same functional dependence on K as does subcritical velocity. However, as shown by Nadeau [131] this acoustic emission is caused by interaction between the moving crack and defects on the surface. (This raises the possibility of correlation between acoustic emission bursts and Wallner lines.) No such interaction is expected for Hertzian cone cracks, and as a matter of fact the results of Swindlehurst and Wilshaw [132] show that a single Hertzian cone produces a single emission burst, most probably when the maximum of G, in Fig. 9 of the companion paper [133], reached G_c. Presumably, for cones formed at subcritical velocity no acoustic emission would be detected. Our preliminary investigations on this point seem to confirm this idea.

8. Embrittlement and the Rehbinder effect

Let us consider a SEN or a DCB specimen under a dead load P (unstable geometry) that gives a subcritical crack ($G < G_c$) very slowly moving along the first positive branch as the crack length increase (Point I on Fig. 22). Put this specimen in a liquid that lowers the surface energy, has no corrosive effect (supersaturated in the components of the solid) and

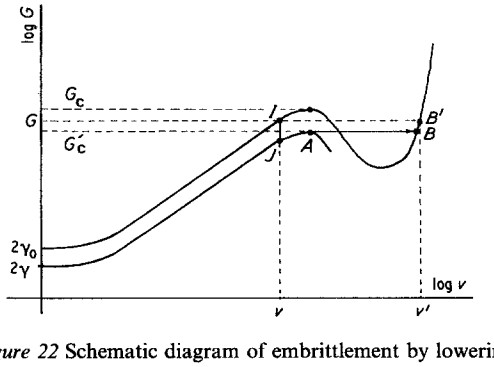

Figure 22 Schematic diagram of embrittlement by lowering surface energy (Rehbinder effect).

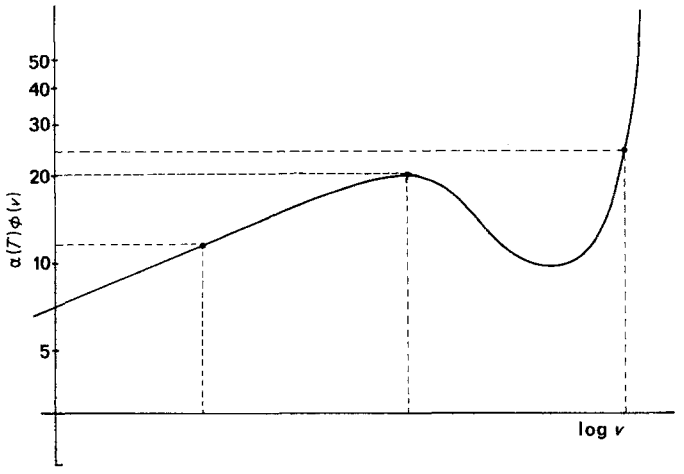

Figure 23 Numerical example for Rehbinder effect.

whose viscosity is such that it can follow the crack tip without drag up to the critical velocity v_c. When the liquid reaches the crack tip, it lowers the surface energy of the nascent surfaces by $\Delta\gamma$ and the representative Point J is on the shifted curve. If G is now higher than G_c' the crack speed jumps onto the second positive branch (after some incubation time), following the path $JABB'$. A small reduction in surface energy by adsorption leads to catastrophic failure at a load which otherwise gave no apparent effect. This is the essence of the Rehbinder effect. This effect is not due to an increase in the driving force $G - 2\gamma$ by $2\Delta\gamma$, but to a drastic reduction to crack resistance on the RHS of Equation 27, and $\phi(v)$ must considerably increase to restore the balance.

Let us take a numerical example with $G = 10\,J\,m^{-2}$, $\gamma_0 = 0.4\,J\,m^{-2}$, $\gamma = 0.2\,J\,m^{-2}$ and consider the curve $\alpha\phi(v) = (G - 2\gamma)/2\gamma$ (Fig. 23) whose maximum at v_c is 20. For $\gamma_0 = 0.4$ the value $\alpha\phi(v)$ is 11.5 and the propagation is subcritical. For $\gamma = 0.2\,J\,m^{-2}$, its value is 24 and the propagation is catastrophic. If γ reaches only $0.25\,J\,m^{-2}$ the value is 19, and after some "incubation time" during which the crack advances ($\partial G/\partial A$ is negative) until v_c is reached, a catastrophic failure appears. (Such experiments of delayed failure have been performed by Bryukhanova *et al.* [134] and Westwood and Kamdar [135] with zinc embrittled by mercury, or cadmium by gallium). If the stress σ at brittle rupture ($G = G_c$) is measured in various liquids, one will have from Equation 29

$$\frac{\sigma_0^2 - \sigma^2}{\sigma_0^2} = \frac{\Delta\gamma}{\gamma_0} \qquad (33)$$

where $\Delta\gamma$ is the reduction of surface energy given by the Gibbs equation, Equation 30. This fact has added still more confusion about the Griffith criterion, since the equation $G_c = 2\gamma$ seems to be confirmed by Equation 33. The confusion simply arises because γ_r is proportional to γ. The ratio $\eta = \gamma/\gamma_0$ thus appears as an embrittling efficiency [136].

So far, we have assumed a deep minimum in the curve, so that the crack speed can jump onto the second stable branch of the virgin material, with no necessity for the embrittling medium to follow the crack at this velocity. Such a material can be said to be *notch brittle* (bcc metals and zinc). If on the contrary the minimum is shallow (Fig. 24), propagation is rapid so long as active medium can feed the crack, and the crack will stop if the supply of active medium is exhausted (as shown by Stoloff and Johnston [137]) for *notch insensitive* metals (fcc and cadmium). Increasing the external pressure increases the limit velocity for cavitation according to Equation 32, and as a result the crack propagates more rapidly. This effect was observed by

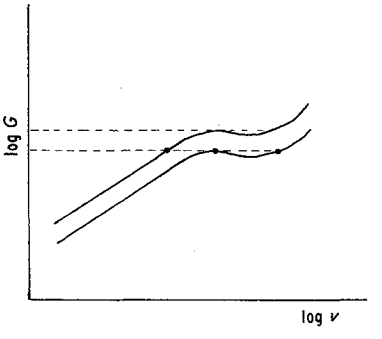

Figure 24 Assumed log G–log v curves for notch-insensitive materials.

Rhines *et al.* [138]. This delicate balance of factors (crack tip feeding, viscosity, cavitation speed, position of the maximum and minimum of the $\phi(v)$ curve) which change with temperature, explains why prediction of embrittlement effects are impossible from purely chemical considerations, and so hazardous on uninvestigated systems.

These embrittling effects due to reduction of intrinsic surface energy by adsorption from gases or liquids, or by segregation of impurities at grain boundaries, are very general and have given rise to a vast literature. These effects were particularly studied by the Rehbinder school (Rehbinder, Likhtman, Shchukin and co-workers) since 1928 but, as quoted by Westwood [139], embrittlements of solid metals by liquid metals were first reported by Huntington [140] and Heyn [141] in 1914. A number of reviews have been published, either general [136, 139, 142–147] or limited to liquid metal embrittlement [136, 148–155] or to embrittlement by grain-boundary segregation [156–160]. We will examine some examples.

As reported by Rehbinder and Shchukin [142, 143] Kontorovitch and co-workers have studied the fracture of porous samples of magnesium hydroxide (obtained by hydratation hardening of magnesium oxide) at various relative humidities. The large specific surface (tens of $m^2 g^{-1}$ measured by the BET method) makes it possible to determine the adsorption Γ by a gravimetric method, and to compute the reduction $\Delta\gamma$ of intrinsic surface energy by the Gibbs formula (Equation 30). Moreover, nuclear magnetic resonance experiments showed that water was present in the form of an adsorption layer, and not in the form of a liquid phase (hence no menisci and an absence of dissolution). They measured the stress σ at fracture (connected with the rupture of bridge contact between particles) at various relative humidities and plotted $(\sigma_0^2 - \sigma^2)/\sigma_0^2$ against $\Delta\gamma$ (Fig. 25). The result clearly verified Equation 33 and the slope gave the value $\gamma_0 = 0.3\,J\,m^{-2}$, so that embrittling efficiency was $\eta \simeq 0.3$ at the higher vapour pressures.

Skovrtsov *et al.* [161] measured the "surface energy" γ of naphthalene single crystals by cleavage in various liquids at fixed cross-head velocity $\dot{\Delta} = 4\,mm\,sec^{-1}$ and compared it to the fracture stress σ of naphthalene polycrystals

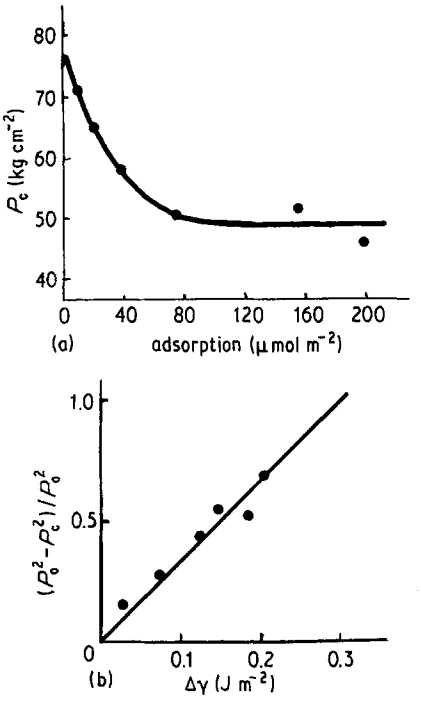

Figure 25 Embrittlement of magnesium hydroxide: (a) Decrease of strength with water adsorption, (b) Comparison between observed reduction of strength and reduction of surface energy independently computed by the Gibbs equation (from [142]).

in the same liquids. Plotting $(\gamma/\gamma_0)^{1/2}$ against σ/σ_0 they claimed to have verified Equation 33. This raises criticisms: the two methods belong to fracture mechanics and the use of such ratios, eliminating numerical factors, will always give $(\gamma/\gamma_0)^{1/2} = (\sigma/\sigma_0)$ even if such an important effect as the storage of elastic energy in the uncleaved part of the crystal was neglected (as pointed out in [162]). More interesting is the variation of strength of polycrystalline samples of naphthalene in aqueous solutions of alcohols of the saturated series as a function of the concentration as reported by Rehbinder and Shchukin [142, 143], and given in Fig. 26. The authors claimed to have verified Traube's rule for variation in surface activity in homologous series. Briefly, in an ideal dilute solution, the chemical potential of the solute varies with the concentration as

$$\mu = \mu_0 + RT \ln c \qquad (34)$$

so that the Gibbs equation

$$d\gamma = -\Gamma d\mu \qquad (35)$$

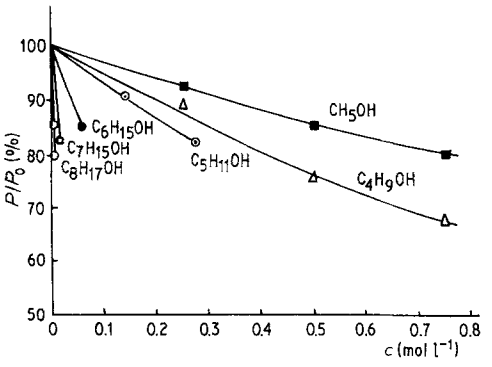

Figure 26 Relative decrease of the strength of polycrystalline naphthalene samples in aqueous solutions of alcohols of the saturated series as a function of concentration (from [142]).

gives

$$\frac{d\gamma}{dc} = -\frac{\Gamma RT}{c} \tag{36}$$

which for $c \to 0$ is the surface activity [163]. Assuming a Langmuir-type adsorption

$$\Gamma = \Gamma_{Max} \frac{c \exp(-\Delta G/RT)}{1 + c \exp(-\Delta G/RT)} = \Gamma_{Max} \frac{ac}{1 + ac} \tag{37}$$

where ΔG is the free energy of adsorption, Equation 36 gives

$$\Delta\gamma = -RT\Gamma_{Max} \ln(1 + ac) \tag{38}$$

so that, assuming Γ_{Max} = constant, equal values of ac give equal values of $\Delta\gamma$. The empirical Traube's law states that for each additional CH_2 group, the concentration required to give a certain surface energy to the dilute solution is reduced by a factor of three (e.g. [163, 164]). If so, the concentration corresponding to a given lowering of strength should decrease by a factor of three between two succeeding homologues. Although this is not very evident in Fig. 26, this example is interesting for its analogy with embrittlement with grain boundary segregation.

When a metal containing impurities is heated, segregation occurs to the surface and to grain boundaries (GB) to reduce surface energy and GB energies, according to the Gibbs equation. The situation is similar to the adsorption of impurities at surface or interface in liquids, but the kinetics of segregation, governed by the McLean equation [165, 166] is much slower than in liquids. When equilibrium is reached the segregated atoms can form a monolayer or multilayers, and several adsorption isotherms can be proposed as for adsorption on to a surface [167]. For example the McLean adsorption relation

$$\frac{\Gamma_b}{\Gamma_{b_{Max}} - \Gamma_b} = \frac{c}{1 - c} \exp(-\Delta G_b/RT) \tag{39}$$

is similar to the Langmuir Equation 37, if the term c in the denominator is negligible. Surface energy can be measured by zero creep experiments, and GB energies deduced from the dihedral angle formed by thermal etching where the GB intersects the free surface [168]. From the variation of surface and GB energies with the bulk impurity level, the segregations Γ_s and Γ_b can be deduced by the Gibbs equation. Γ_s and Γ_b can also be directly measured by Auger electron spectroscopy examination of the surface or the GB after intergranular rupture in a vacuum [169].

Most of the studies have been done on steel, and on interaction between co-segregating species causing temper brittleness, and the results are very impressive [159]. Fewer papers have been published on the variation of stress to rupture with the variation of γ_s and γ_b. Fig. 27 (from Hondros and McLean [170]) compares the variation of ultimate tensile stress and GB energy with the bulk bismuth content in copper. Such intergranular rupture is quite similar to the adherence problem, and is related to the Dupré energy of adhesion as first proposed by Inman and Tipler [171]:

$$w = 2\gamma_s - \gamma_b$$

However, two difficulties arise with the thermodynamics of w. Firstly, the Gibbs equation implies that both γ_s and γ_b are reduced by segregation, but nothing is said about w. If γ_b decreases more rapidly than γ_s, w can eventually increase with segregation. Secondly, as pointed out by Inman and Tipler [171], the surface energy of the newly formed crack surface can be different from the equilibrium surface energy γ_s. Assuming a very dilute solution ($ac \ll 1$) so that Equations 37 and 38 give $\Delta\gamma = -\Gamma RT$, Seah [157, 158] wrote

$$w = 2\gamma_s^0 - 2\Gamma_s RT - \gamma_b^0 + \Gamma_b RT$$

or

$$w = w_0 - RT(2\Gamma_s - \Gamma_b) \tag{40}$$

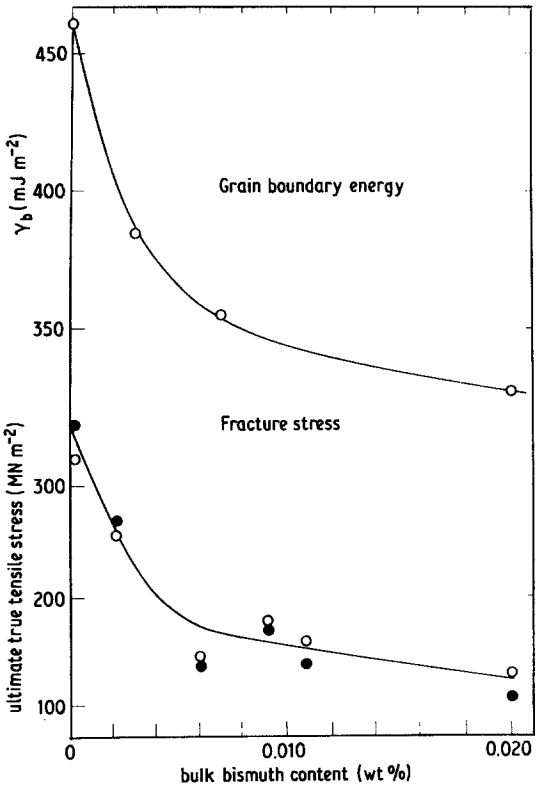

Figure 27 Dependence of grain boundary energy and ultimate tensile strength of copper on bismuth content: ● fast test; ○ slow test (from [170]).

For slow fracture at high temperature Γ_s can be the equilibrium value, so that w generally decreases with segregation, but he pointed out that for fast fracture at low temperature, Γ_b is divided on the two surfaces to give a surface segregation $\Gamma'_s = \frac{1}{2}\Gamma_b$, so that Equation 40 would give no variation in Dupré energy of adhesion, even in embrittled system. This result was in complete disagreement with previous ideas on embrittling effects, and Seah [158] proposed that embrittlement is related to the excess size of the segregant atoms over those of the matrix.

The problem with Equation 40 was solved by Hirth and Rice [172]. Fig. 28 displays the variation of $2\gamma_s$ and γ_b with the chemical potential μ of the impurity, assuming Langmuir-type segregation. The slopes of these curves give $2\Gamma_s$ and Γ_b according to Equation 35. For a quasistatic crack propagation at a given μ, the surface and GB segregations are represented by Points K and L, and surface and GB energies by Points A and B, and the Dupré work of adhesion by AB.

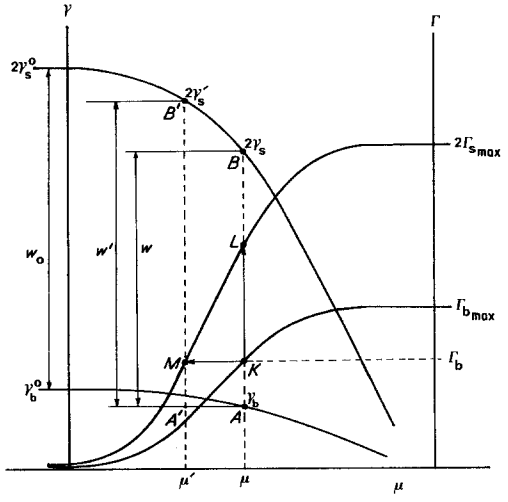

Figure 28 Variation of twice surface energy, grain boundary energy, and adsorption with chemical potential of the impurity, assuming Langmuir-type segregation.

For a fast fracture, one has $\Gamma_s = \frac{1}{2}\Gamma_b$ (Point M) and assuming local thermodynamic equilibrium, the surface energy $2\gamma'_s$ corresponds to Point B' as for a chemical potential μ', and the Dupré energy of adhesion to $A'B' = w'$. Hirth and Rice [172] have shown that this new Dupré energy of adhesion is

$$w' = w_0 - (\mu - \mu')\Gamma_b \qquad (41)$$

Using Equation 37 for Γ_b (at concentration c) and $\Gamma_s = \frac{1}{2}\Gamma_b$ (at concentration c'), and assuming $\Gamma_{b_{Max}} = \Gamma_{s_{Max}}$, it becomes

$$w' = w_0 + \Gamma_b RT\left(\frac{U}{RT} - \ln 2\right) \qquad (42)$$

with

$$U = \Delta G_s - \Delta G_b = \Delta H_s - \Delta H_b - T(\Delta S_s - \Delta S_b) \qquad (43)$$

as given by Seah [173]. Similar treatment on Equation 40 gives

$$w = w_0 + \Gamma_b RT\left[1 - 2\exp\left(-\frac{U}{RT}\right)\right] \qquad (44)$$

In both cases the Dupré energy of adhesion is linearly dependent on the level of segregation, and decreases with segregation if $\Delta G_s - \Delta G_b < RT \ln 2$, but less rapidly for fast fractures (Fig. 29). Seah [173] using a pair bonding

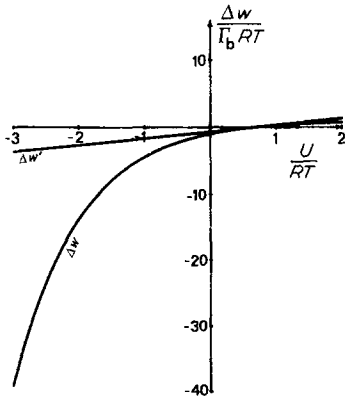

Figure 29 Reduction of Dupré energy of adhesion with $U = \Delta G_s - \Delta G_b$ for fast and slow fracture.

approach found Equation 42 directly (neglecting entropic terms in Equation 43), and showed that $w_0 - w'$ is proportional to the difference $H_A^{sub*} - H_B^{sub*}$ in sublimation enthalpy of pure matrix and impurity per unit area, so that the remedial or embrittlement effect of segregant atoms can be predicted from standard texts of thermodynamic data. Fig. 30 (from Seah [173]) shows these sublimation enthalpies as a function of atom size. Taking any element as the matrix, elements lower in the figure will, if segregated, cause embrittlement of the matrix GB, whereas elements highter will be remedial to such embrittlement. Roughly, small-radius atoms increase the GB cohesion, large-radius atoms decrease it. Such a map is also a good guide for adhesion and welding problems. The results reported here show how closely fracture mechanics is related to chemistry.

9. Fracture surface energy of metals

Ductile fracture and the ductile–brittle transition are outside the scope of this paper, but the key to brittle-fracture mechanics is certainly the relationship between surface energy or Dupré energy of adhesion and the dissipative processes. This fact has been pointed out repeatedly for thirty years. Let us return for a while to the early age of fracture mechanics, and follow the evolution of ideas.

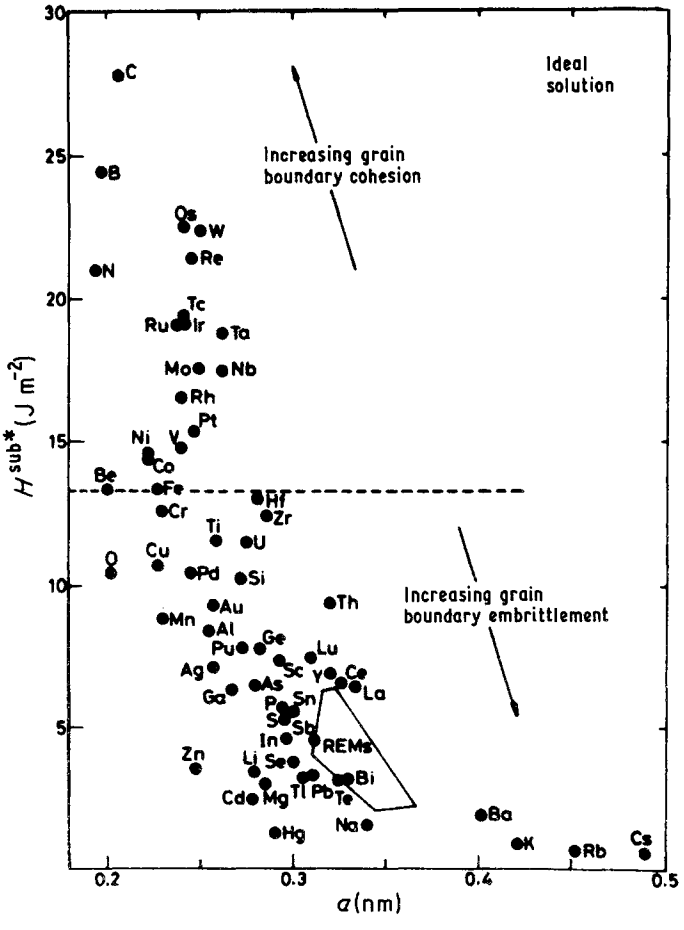

Figure 30 Plot of sublimation enthalpies against atom size, giving a guide for the remedial/embrittlement effect of segregated atoms (from [173]).

In his famous paper in 1920, Griffith [174] computed the increase of strain energy in a plate containing an elliptical crack of length $2c$ and, introducing for the first time the surface energy of solids in mechanics, wrote that at equilibrium the total energy of the plate was an extremum:

$$\frac{\partial}{\partial c}(U_E - 4\gamma c) = 0$$

i.e.

$$\sigma \simeq \left(\frac{\gamma E}{c}\right)^{1/2} \quad (45)$$

In this geometry, the extremum is a maximum and equilibrium is unstable. The condition of Equation 45 is thus a condition that the crack may extend, taking the energy for increasing the crack area from the elastic field. In 1945, Orowan [175] gave Griffith criterion by a very simple argument. Approximating the force law between atoms by a sine curve, he estimated the theoretical strength of materials to be

$$\sigma_{th} \simeq \left(\frac{E\gamma}{a_0}\right)^{1/2} \quad (46)$$

where a_0 is the interatomic distance. Comparing with the Inglis formula for maximum stress σ_c at the end of an elliptical crack of length $2c$ and radius of curvature ϱ,

$$\sigma_c = 2\sigma\left(\frac{c}{\varrho}\right)^{1/2} \quad (47)$$

and assuming $\sigma_c = \sigma_{th}$ and $\varrho = a_0$ at a crack tip, he found thus the Griffith criterion from local conditions at the crack tip. The two ways to attack fracture mechanics, by an energy approach or by a stress intensity approach, where shown. In 1952, Irwin and Kies [176] introduced the strain energy release rate G, and in 1954 [177] the compliance methods to measure it. By a semi-inverse method, Westergaard [178] had shown in 1939 that the elastic solution for a crack gave an elliptic shape with stress singularities at the edge, and the leading terms of the stress tension near the edge of a crack were given by Sneddon [179] in 1946. In 1957 Irwin [180], introducing the stress intensity factor (later denoted K [181]) to describe the magnitude of the stress singularities, showed that the strain energy release rate, which he also called crack extension force, was the work done by the singular stresses to close the elliptical crack, and thus placed the equivalence between energy and stress intensity approaches on a higher level of understanding. Modern fracture mechanics was born.

The application of Griffith's criterion to fast fracture in metals was initially questioned. In 1949, Orowan [182] wrote: "In ductile fracture, the work done against the cohesive forces is usually negligible compared with the work of plastic deformation that has to be done in order to extend the crack", and in a footnote "The plastic work p per unit area must be added to the surface energy α in Griffith's equation; in fact the order of magnitude of p (10^6 to 10^7 erg cm^{-2}) is higher than that of surface energy (10^3 erg cm^{-2}), so that the latter can be neglected and, instead of Griffith's equation, the condition $\sigma = (pE/c)^{1/2}$ used". Similarly, Irwin [183] suggested that the Griffith theory could be made generally applicable by substitution of energy spent in localized plastic strain for surface energy as a measure of resistance to crack extension, and the modified Griffith formula

$$\sigma \simeq \left(\frac{\gamma_p E}{c}\right)^{1/2} \quad (48)$$

became known as Irwin–Orowan formula. Irwin [181] introduced the critical value G_c, noting that "Since the change from slow to fast fracturing of a developing crack is usually abrupt, fracture strength may be described as the critical value G_c of the crack extension force, G, necessary for onset of rapid crack extension". Later much confusion arose with G_c, some authors using it for the Griffith criterion $G_c = 2\gamma$ others as $G_c = 2\gamma_f$ for onset of rapid propagation, others for any detectable crack velocity in the subcritical range. Even Strawley and Brown [184] wrote "In some of the literature on fracture mechanics, G_c is defined in different terms, for instance, as the value of the crack extension force at onset of rapid crack propagation. Such a definition is too vague as an operational definition for testing purposes, and may be even misleading in seeming to imply that continuing slow crack extension is to be expected at constant levels of G less than G_c. Such behaviour fortunately is unusual", and they proposed to define it from the maximum recorded load and the corresponding crack length in an experiment at fixed cross-head velocity. This fourth definition is the analogue of tack force in adherence, and as discussed above has no simple physical significance.

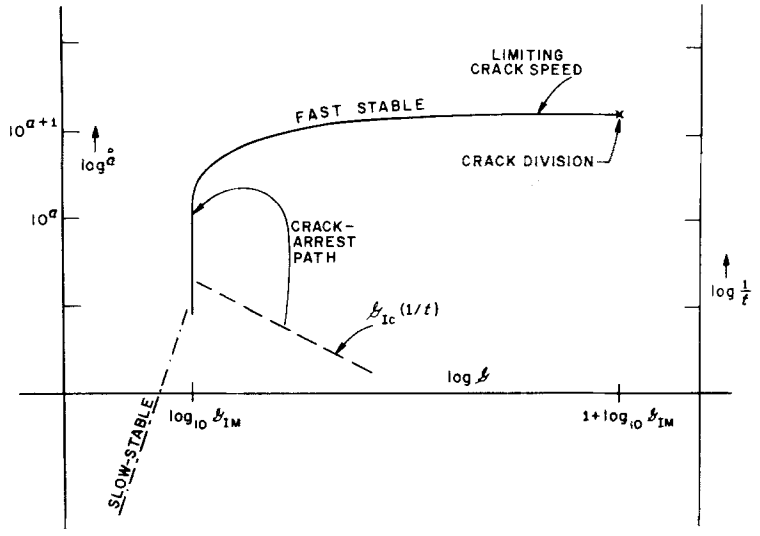

Figure 31 Crack extension behaviour as a function of strain energy release rate (from [185]). "The solid curve and the dash-dot curve show the fast-stable and slow-stable regimes in term of log (crack speed) as a function of log G. The vertical line segment forming the lower left portion of the solid curve represents the tendency of crack arrest, in rate-sensitive materials, to occur abruptly from a certain minimum velocity. This vertical portion should be thought of as a stretched-out end-point of the fast stable regime. Crack extension is stable only where the slope of line is positive and finite. In terms of a loading-speed scale at the right of the graph, $\log(1/t)$, the dashed line represents the tendency of G_{Ic}, for onset of rapid fracture, to decrease with increase of strain rate". [185]. Clearly, the vertical solid line is similar to the line CD of Fig. 13, and the dashed line is similar to the variation of K_{Ici} with cross-head velocity in Fig. 17.

On the other hand Irwin and Paris [185] wrote in 1971: "In terms of the old modified Griffith theory (Irwin–Orowan), the condition critical for the onset of rapid fracture was a point of stable balance, between stress field energy release rate and rate of plastic work, to be followed by a regime of unstable rapid propagation. However, study of the implications from Well's thermal measurements suggested, quite oppositely, that the point of rapid fracture was an abrupt instability point followed by a stable regime in which work rate and loss of stress field energy were balanced through a considerable range of crack speeds. Indeed, the instability point could be preceded by a slow regime of crack extension in which the crack extension process was also stable." They gave a schematic diagram (Fig. 31) quite similar to Fig. 13. The model proposed here is thus very general.

It is evident that the question of the relationship between surface energy or Dupré energy of adhesion and the magnitude of dissipative processes should have been raised by researchers working on segregation or liquid embrittlement, who were familiar with the Gibbs equation. Indeed, the question was raised by McLean [165] who wrote in 1957: "If the energy of the surface along which fracture is to spread is small, the tensile stress concentration required at the tip of the crack to start or continue fracture is also small. The associated shear stress concentration, which produces the plastic deformation is therefore also small and little plastic work is done. Hence the plastic deformation work done is governed by the energy of the fracture surface." The same argument has been presented repeatedly, and was used by Andrews and Kinloch [18] for viscoelastic losses. In 1963, Stoloff and Johnston [137] suggested following the Orowan [175] derivation of the Griffith criterion from Equations 46 and 47, still assuming $\sigma_c = \sigma_{th}$ at the crack tip, but with $\varrho \neq a_0$ to take into account the alteration of shape due to plastic deformation (crack blunting). They thus obtained

$$\sigma \simeq \left(\frac{E\gamma}{c}\frac{\varrho}{a_0}\right)^{1/2} \tag{49}$$

and proposed to identify $\gamma\varrho/a_0$ with the γ_p of the Irwin–Orowan formula (Equation 48), so that plastic deformation does not provide an energy term added to γ but a dimensionless ratio which multiplies γ. They were followed by Westwood and Kamdar [135]. By a dimensional analysis, Rice

[186] showed in 1965 that "at fracture the energy release rate is directly proportional to the surface energy term as multiplied by some function f depending on material constants describing the elastic–plastic behaviour". Assuming simultaneous bond breaking and dislocation emission at the crack tip, McMahon and Vitek [187] proposed that γ_p varies as γ^n with $n \simeq 7$, and later [188] with n between 1 and 2. In this last case, n is related to the power law dislocation velocity

$$v = v_0 \left(\frac{\tau}{\mu}\right)^n$$

where τ is the local stress and μ the shear modulus. The problem with metals is to find a microscopic mechanism leading to a negative resistance branch at high stresses or high strain rates.

10. Conclusion

In this paper, we have attempted to extend and generalize our ten years' experience on adherence of solids to some general problems of fracture mechanics. The theory of adherence of punches on elastic solids is firmly established from the three points of view of mechanics of contact, fracture mechanics and general theory of elasticity. Equilibrium cracks, crack healing and the kinetics of crack propagation have been studied for various glass–elastomer contacts, and the general equation

$$G - w = w\phi_T(v)$$

was found to explain all the results and to give precise predictions. $\phi_T(v)$ is related to viscoelastic losses at the crack tip. As viscoelastic losses generally decrease at high frequency, it was assumed that the function $\phi(v)$ can decrease at higher crack velocities. However, a $\phi(v)$ branch with a negative slope cannot be observed, for it corresponds to resistance decreasing as the crack velocity increases, and velocity jump or stick–slip must be observed depending on the geometry tested. It was felt that the value of G (or K) at which the velocity jump occurs was the G_c (or K_c) of fracture mechanics, so that crack propagation below G_c (subcritical crack growth) is a normal propagation according to the Griffith criterion, and needs no stress corrosion to explain it. Moreover the multiplicative factor w gives a shift of the $v-K$ curves with environment, which could explain embrittlement by reduction of G_c when the surrounding medium can still reach the crack tip at the velocity corresponding to velocity jump.

With these ideas in mind, the literature concerning fracture of glasses, ceramics and brittle polymers was reviewed together with that for stick–slip, the Rehbinder effect and embrittlement by segregation. When the pieces of that puzzle are assembled, a very simple picture of fracture mechanics emerges, with stable slow crack propagaton for $2\gamma < G < G_c$ and stable fast propagation for $G > G_c$. It is pointed out that the definition of G_c by the maximum recorded force in an experiment at constant cross-head velocity is not correct, since the maximum can be reached at subcritical velocity. Occurrence of velocity jump or stick–slip depends on the geometry tested and the stiffness of the apparatus, as expected. The shift of $v-K$ curves with adsorption seems in agreement with the predicted reduction in surface energy, and the ratio of surface energies in various environments can be deduced from the ratio of strain energy release rates taken at the same crack velocity. When the surrounding medium can reach the crack tip and reduce the surface energy of the nascent surfaces, even at the critical velocity where the velocity jumps, the critical strain energy release rate G_c is reduced in the same proportion as γ, and a loading which would have given a subcritical crack growth will give a catastrophic failure, Incubation time, which was a stumbling block for the explanation of the Rehbinder effect by reduction of surface energy, appears here naturally. Embrittlement by segregation is very similar to the Rehbinder effect, except for the viscous effect and for the fact that Dupré's energy of adsorption can decrease or increase by adsorption, whereas surface energy always decreases.

Most of the ideas proposed here are not new and have been given here and there in the literature (e.g. static fatigue limit corresponding to intrinsic surface energy, fracture toughness related to the transition from slow to fast propagation, stick–slip due to a negative-resistance branch, losses at crack tip proportional to surface energy) but when put together they lead to a single model that accounts for a number of phenomena not hitherto related to each other. The central points of that theory

are (a) the proportionality between surface energy or Dupré energy of adhesion and losses at the crack tip, and (b) the existence of a branch $\phi(v)$ with a negative slope between two branches with positive slopes. There are good experimental clues but no firm theory. We have tried to follow the evolution of idea concerning the relation between γ and γ_p in the Irwin–Orowan formula; this question is still an evergreen topic. For viscoelastics we can hope that the function $\phi(v)$, with its negative branch, will be in the future directly derived from the variation of E' and E'' with frequency. For metals the existence of a negative-resistance branch is more puzzling, and the ductile–brittle transition is not yet clear.

If a few recommendations for future work can be made, the following are proposed: (a) study the whole v–K curve, since K_c (or G_c) is only one point on that curve; (b) be careful with experiments at fixed cross-head velocity, because the recorded force can be difficult to interpret; (c) studies of viscous drag and the variation of cavitation with external pressure would be of interest; (d) a study of the embrittlement effect should involve study of subcritical crack growth to see if the whole v–K curve is shifted; (e) compare the variation of γ with the variation of G at the same crack velocity.

We have noted that experiments on embrittlement, although of high standard in physical chemistry, are not of the same standard as fracture mechanics experiments on glasses: too many workers still use mean stress at rupture, instead of G or K which allow comparison between various geometries.

Acknowledgements

The author is indebted to GRECO 46 and DRET for financial support.

Appendix: Velocity jump and stick–slip in DCB tests

In its simpler form (neglecting shear stresses and rotation of section at the crack tip) the relation between load and displacement (Fig. A1) is

$$\delta = 2\frac{4PL^3}{Ebh^3} \tag{A1}$$

and hence the stiffness is

$$k = \left(\frac{\partial P}{\partial \delta}\right)_A = \frac{Ebh^3}{8L^3} \tag{A2}$$

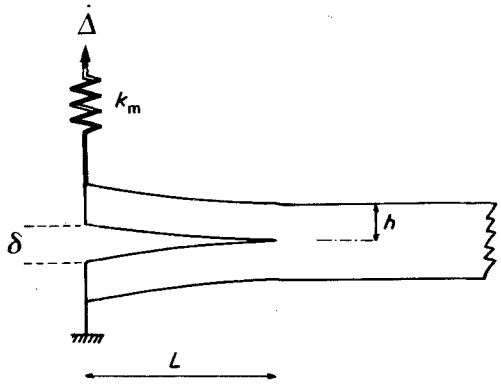

Figure A1 DCB specimen – k_m represent the stiffness of the testing apparatus.

After evaluation of elastic energy, the strain energy release rate is

$$G = \frac{12P^2L^2}{Eb^2h^3} = \frac{3Eh^3\delta^2}{16L^4} \tag{A3a}$$

or using Equations 18 and A1

$$G = \frac{3Eh^3}{16L^4}\frac{\Delta^2}{\left(1 + \dfrac{Ebh^3}{8k_mL^3}\right)^2} \tag{A3b}$$

Equations A1 and A3a are the equations of state (Equations 2b and c) of the system. The Maxwell relations (Equations 6 and 7) give

$$\left(\frac{\partial G}{\partial \delta}\right)_A = \left(\frac{\partial P}{\partial A}\right)_\delta = \frac{3Eh^3\delta}{8L^4} = \frac{3P}{bL} \tag{A4}$$

$$\left(\frac{\partial G}{\partial P}\right)_A = -\left(\frac{\partial \delta}{\partial A}\right)_P = \frac{24PL^2}{Eb^2h^3} = \frac{3\delta}{bL} \tag{A5}$$

where $dA = -b dL$, and Equation 8 is verified.

Equilibrium is unstable at fixed load, and stable at fixed grips since

$$\left(\frac{\partial G}{\partial A}\right)_P = -\frac{24P^2L}{Eb^3h^3} < 0 \tag{A6}$$

$$\left(\frac{\partial G}{\partial A}\right)_\delta = \frac{3Eh^3\delta^2}{4bL^5} > 0 \tag{A7}$$

The condition for stability at fixed cross-head displacement Δ, derived from Equation 17 or

directly from Equation A3b, is

$$\left(\frac{\partial G}{\partial A}\right)_{\Delta} = \frac{3Eh^3\delta^2}{4bL^5} \times \left[1 - \left(\frac{3Ebh^3}{16L^3}\right)\frac{1}{k_m + \frac{Ebh^3}{8L^3}}\right] > 0 \quad \text{(A8)}$$

so that the condition for stable equilibrium is

$$k_m > \frac{Ebh^3}{16L^3} \quad \text{(A9)}$$

Letting L_0 be the initial crack length, Δ_0 the equilibrium cross-head displacement, and $k_0 = Ebh^3/8L_0^3$, Equation A3b becomes

$$\frac{G}{2\gamma} = \left(\frac{\Delta}{\Delta 0}\right)^2\left(\frac{L_0}{L}\right)^4 \times \left[\frac{1 + (k_0/k_m)}{1 + (k_0/k_m)(L_0^3/L^3)}\right]$$

and is given in Fig. A2 for $k_m = 0.1$, 1 and 10 k_0, and for various imposed cross-head displacements. In the first case equilibrium under Δ_0 is unstable, and the crack first accelerates and then slows down with an inflexion point in between. For various imposed values of Δ, the inflexion point occurs at the same crack length L corresponding to equality in Equation A9. The situation is quite similar to what is observed with the adherence of a sphere [2, 3] or the Hertzian fracture [133].

However, at fixed cross-head velocity $\dot{\Delta}$ the problem is more complicated, for the crack is never in equilibrium. Differentiating Equation 18, the relation between $\dot{\delta}$ and $\dot{\Delta}$ during crack propagation is

$$\dot{\delta} = \left[\dot{\Delta} - \frac{1}{k_m}\left(\frac{\partial P}{\partial A}\right)_{\delta}\dot{A}\right] \Big/ \left[1 + \frac{1}{k_m}\left(\frac{\partial P}{\partial \delta}\right)_A\right] \quad \text{(A10)}$$

which correctly gives $\dot{\delta} = \dot{\Delta}$ for $k_m = \infty$ and $\dot{\delta} = (\partial\delta/\partial A)_P\dot{A}$ for $k_m = 0$ (using Equation 8). When the machine is stopped (load relaxation technique), Equation A10 together with

$$\dot{\delta} = \left(\frac{\partial \delta}{\partial P}\right)_A \frac{dP}{dt} + \left(\frac{\partial \delta}{\partial A}\right)_P \dot{A}$$

gives

$$\dot{A} = \left(\frac{\partial A}{\partial P}\right)_{\delta}\left[1 + \frac{1}{k_m}\left(\frac{\partial P}{\partial \delta}\right)_A\right]\frac{dP}{dt} \quad \text{(A11)}$$

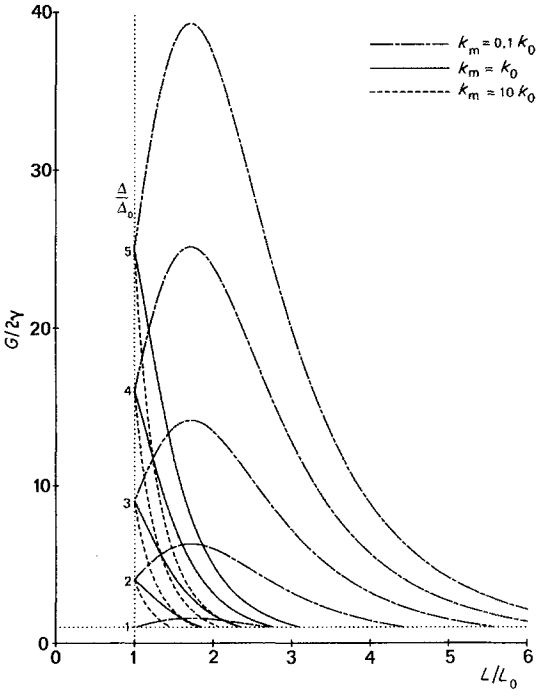

Figure A2 Reduced strain energy release rate against reduced crack length, at various imposed cross-head displacements, for DCB tested with apparatus of various stiffnesses.

i.e. for a DCB test

$$v = -\frac{L}{3P}\left[1 + \frac{Ebh^3}{8k_mL^3}\right]\frac{dP}{dt} \quad \text{(A12)}$$

On the other hand, if the load is continuously recorded at $\dot{\Delta}$ = constant, one has

$$\frac{dP}{dt} = \left(\frac{\partial P}{\partial \Delta}\right)_A\dot{\Delta} + \left(\frac{\partial P}{\partial A}\right)_{\Delta}\dot{A} = \left(\frac{\partial P}{\partial \Delta}\right)_A\left[\dot{\Delta} - \left(\frac{\partial \delta}{\partial A}\right)_P\dot{A}\right] \quad \text{(A13)}$$

i.e. for DCB

$$\frac{dP}{dt} = \frac{Ebh^3}{8L^3}\left(1 + \frac{Ebh^3}{8k_mL^3}\right)^{-1} \times \left(\dot{\Delta} - \frac{3\delta}{L}v\right) \quad \text{(A14)}$$

When v is small P increases, and when v becomes high P decreases. The maximum of P thus occurs at a velocity v depending on the geometry of the specimen and on $\dot{\Delta}$, and does not generally correspond to v_c and G_c. At this

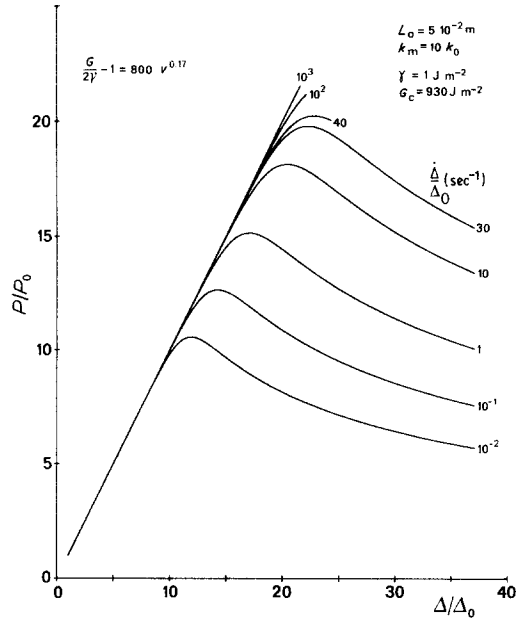

Figure A3 Computed curves of recorded load against cross-head displacement at various cross-head velocities, for a DCB specimen of PMMA. At low cross-head velocities G_C is never reached, and P_{max} corresponds to subcritical crack growth.

stage the velocity v is not known. It depends on G (Equation 27) which varies with time according to

$$\frac{dG}{dt} = \left(\frac{\partial G}{\partial \Delta}\right)_A \dot{\Delta} + \left(\frac{\partial G}{\partial A}\right)_\Delta \dot{A} \qquad (A15)$$

with $(\partial G/\partial A)_\Delta$ given by Equation A8 and

$$\left(\frac{\partial G}{\partial \Delta}\right)_A = \left[1 + \frac{1}{k_m}\left(\frac{\partial P}{\partial \delta}\right)_A\right]^{-1} \left(\frac{\partial G}{\partial \delta}\right)_A \qquad (A16)$$

For DCB the curve $P(t)$ can be numerically computed, using Equations, A14, A3b and 27.

Fig. A3 is for a DCB specimen ($L_0 = 5 \times 10^{-2}$m, $k_m = 10\ k_0$) of PMMA ($E = 2.9 \times 10^9$ Pa) and taking $\gamma = 1\,\mathrm{J\,m^{-2}}$, $G_c = 930\,\mathrm{J\,m^{-2}}$

$$\frac{G}{2\gamma} - 1 = 800\, v^{0.17}$$

which closely fits the experimental results of Marshall *et al.* [90] on subcritical crack growth at 20° C. The curves are stopped as soon as G reaches G_c. It clearly appears that P_{max} corresponds to subcritical crack growth at low $\dot{\Delta}$ (note that decreasing G_c decreases the $\dot{\Delta}$ at which velocity jump occurs). If the critical strain energy release rate is computed with Equation A3a (with $k_m = \infty$) from the value of the crack length at P_{max}, the result can be in error for low $\dot{\Delta}$ and low k_m, as shown in Fig. A4.

Note added in proof

A recent paper on the Portevin–Le Chatelier effect (L. P. Kubin, Y. Estrin, *Acta Metall.* **3** (1985) 397) comes to the attention of the author. This effect occurring when dislocations are torn off from their solute atmosphere, and giving a negative strain rate sensitivity, could provide a microscopic mechanism for negative resistance to crack motion in metals. The authors give the stress as

$$\sigma = h\varepsilon + F(\dot{\varepsilon})$$

where h is the work hardening rate, ε the strain, and $F(\dot{\varepsilon})$ a function of the strain rate with a negative branch between two positive ones, and they describe jumps in strain rate and stick–slip motions, in loadings at constant stress rate.

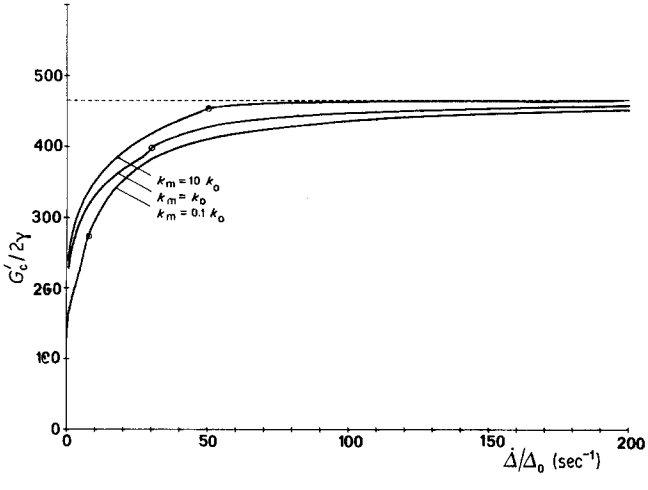

Figure A4 Apparent critical strain energy release rate, computed from P_{max}, with the crack length at P_{max}, (and neglecting k_m), as a function of the cross-head velocity, for apparatus of various stiffnesses. The open circle is for cross-head velocity above which P_{max} corresponds to $G = G_c$.

References

1. D. MAUGIS, "Unilateral problems in structural analysis", CISM courses and lectures series, edited by G. Del Piero and F. Maceri (Springer-Verlag, Berlin, 1985).
2. D. MAUGIS and M. BARQUINS, *J. Phys. D: Appl. Phys.* **11** (1978) 1989.
3. *Idem*, "Adhesion and adsorption of polymers", Part A, edited by L. H. Lee (Plenum Press, New York, 1980) p. 203.
4. M. BARQUINS and D. MAUGIS, *J. Mec. Théor. Appl.* **1** (1982) 333.
5. D. MAUGIS and M. BARQUINS, *J. Phys. D: Appl. Phys.* **16** (1983) 1843.
6. K. L. JOHNSON, K. KENDALL and D. ROBERTS, *Proc. R. Soc.* **A324** (1971) 301.
7. D. MAUGIS, "Microscopic aspects of adhesion and lubrication", edited by J. M. Georges (Elsevier, Amsterdam, 1982) p. 221.
8. G. GURNEY and J. HUNT, *Proc. R. Soc.* **A299** (1967) 509.
9. J. B. OBREIMOV, *ibid.* **A127** (1930) 290.
10. F. C. ROESLER, *ibid.* **B69** (1956) 981.
11. J. D. FERRY, "Viscoelastic properties of polymers" (Wiley, New York, 1970) p. 292.
12. D. H. KAELBLE, *J. Colloid Sci.* **19** (1964) 413.
13. *Idem, J. Adhes.* **1** (1969) 102.
14. A. N. GENT and R. P. PETRICH, *Proc. R. Soc.* **A310** (1969) 433.
15. A. N. GENT, *J. Polym. Sci. A2* **9** (1971) 283.
16. A. N. GENT and A. J. KINLOCH, *ibid.* **9** (1971) 659.
17. A. N. GENT and J. SCHULTZ, *J. Adhes.* **3** (1972) 281.
18. E. H. ANDREWS and A. J. KINLOCH, *Proc. R. Soc.* **A332** (1973) 385.
19. K. KENDALL, *J. Phys. D. Appl. Phys.* **5** (1973) 1782.
20. A. D. ROBERTS, *Rub. Chem. Techn.* **52** (1979) 23.
21. M. BARQUINS, Thèse d'Etat University of Paris, 1980.
22. A. CARRÉ and J. SCHULTZ, *J. Adhes.* in press.
23. A. D. ROBERTS and A. G. THOMAS, *Wear* **33** (1975) 45.
24. M. BARQUINS and D. MAUGIS, *J. Adhes.* **13** (1981) 53.
25. J. W. HUTCHINSON and P. C. PARIS, ASTM STP 668 (American Society for Testing and Materials, Philadelphia, 1979) p. 37.
26. M. BARQUINS, *J. Appl. Polym.* **28** (1983) 2647.
27. *Idem, Int. J. Adhesion and Adhesives* **3** (1983) 71.
28. G. RAMOND, M. PASTOR, D. MAUGIS and M. BARQUINS, *Cah. du Gr. Fr. de Rheol.* in press.
29. R. A. SCHAPERY, *Int. J. Fract.* **11** (1975) 141.
30. R. M. CHRISTENSEN, *ibid.* **15** (1979) 3.
31. R. M. CHRISTENSEN and E. M. WU, *Eng. Fract. Mech.* **14** (1981) 215.
32. M. DAHAN and E. ZNATY, *C.R. Acad. Sci. Paris* **292** Ser. II (1981) 481.
33. J. A. GREENWOOD and K. L. JOHNSON, *Philos. Mag.* **A43** (1981) 697.
34. J. L. GARDON, *J. Appl. Polym. Sci.* **7** (1963) 625.
35. J. R. RICE, *J. Mech. Phys. Sol.* **26** (1978) 61.
36. P. GLANSDORFF and I. PRIGOGINE, "Structure, stabilité et fluctuations" (Masson, Paris, 1971) p. 80.
37. L. GRENET, *Bull. Soc. Encour. Ind. Nat.* **4** (1899) 838.
38. L. H. MILLIGAN, *J. Soc. Glass Technol.* **13** (1929) 351.
39. A. J. HOLLAND and W. E. S. TURNER, *Glass Technol.* **24** (1940) 46.
40. T. C. BAKER and F. W. PRESTON, *J. Appl. Phys.* **17** (1946) 170.
41. S. WIEDERHORN, "Environment sensitive mechanical behaviour", edited by A. R. C. Westwood and N. S. Stoloff (Gordon and Breach, New York, 1966) p. 293.
42. *Idem, J. Amer. Ceram. Soc.* **50** (1967) 407.
43. *Idem, Int. J. Fract.* **4** (1968) 171.
44. S. M. WIEDERHORN and L. H. BOLZ, *J. Amer. Ceram. Soc.* **53** (1970) 543.
45. A. G. EVANS, *J. Mater. Sci.* **7** (1972) 1137.
46. R. J. CHARLES, *J. Appl. Phys.* **29** (1958) 1657.
47. V. P. PUKH, S. A. LATERNER and V. N. INGAL, *Sov. Phys. Sol. State* **12** (1970) 881.
48. S. M. WIEDERHORN, H. JOHNSON, A. M. DINESS and A. H. HEUER, *J. Amer. Ceram. Soc.* **57** (1974) 336.
49. S. M. WIEDERHORN, "Fracture mechanics of ceramics" Vol. 4, edited by R. C. Bradt, D. P. H. Hasselman and F. F. Lange (Plenum, New York, 1978) p. 549.
50. S. W. FREIMAN, "Fracture mechanics of ceramics", Vol. 6, edited by R. C. Bradt, A. G. Evans, D. P. H. Hasselman and F. F. Lange (Plenum, New York, 1983) p. 27.
51. G. W. WEIDMAN and D. G. HOLLOWAY, *Phys. Chem. Classes* **15** (1974) 116.
52. S. M. WIEDERHORN, "Fracture mechanics of ceramics", Vol. 2, edited by R. C. Bradt, D. P. H. Hasselman and F. F. Lange (Plenum, New York, 1974) p. 613.
53. A. G. EVANS, *Int. J. Fract.* **10** (1974) 251.
54. D. P. WILLIAMS and A. G. EVANS, *J. Test. Eval.* **1** (1973) 264.
55. F. CHAMPOMIER and J. C. METRAS, *Verres Refract.* **33** (1979) 858.
56. S. SAKAGUCHI, Y. SAWAKI, Y. ABE and T. KAWASAKI, *J. Mater. Sci.* **17** (1982) 2878.
57. S. M. WIEDERHORN, *J. Amer. Ceram. Soc.* **52** (1969) 99.
58. S. W. FREIMAN, *ibid.* **57** (1974) 350.
59. S. M. WIEDERHORN, E. R. FULLER and R. THOMSON, *Metal Sci.* **14** (1980) 450.
60. G. E. BOYD and H. K. LIVINGSTON, *J. Amer. Ceram. Soc.* **64** (1942) 2383.
61. J. SCHULTZ and H. SIMON, *Verres Refract.* **34** (1980) 192.
62. P. W. R. BEAUMONT and R. J. YOUNG, *J. Mater. Sci.* **10** (1975) 1334.
63. E. J. RIPPLING, S. MOSTOVOY and C. BERSCH, *J. Adhes.* **3** (1971) 145.
64. D. P. HASSELMAN, D. A. KROHN, R. C.

BRADT and J. A. COPPOLA, "Fracture Mechanics of Ceramics", Vol. 2, edited by R. C. Bradt, D. P. H. Hasselman and F. F. Lange (Plenum, New York, 1974) p. 749.
65. E. OROWAN, *Nature* **154** (1944) 341.
66. T. A. MICHALSKE and S. W. FREIMAN, *J. Amer. Ceram. Soc.* **66** (1983) 284.
67. B. J. HOCKEY, "Fracture Mechanics of Ceramics", Vol. 6, edited by R. C. Bradt, A. G. Evans, D. P. H. Hasselman and F. F. Lange (Plenum, New York, 1983) p. 637.
68. S. M. WIEDERHORN and P. R. TOWNSEND, *J. Amer. Ceram. Soc.* **53** (1970) 486.
69. B. R. LAWN, B. J. HOCKEY and S. M. WIEDERHORN, *J. Mater. Sci.* **15** (1980) 1207.
70. B. J. HOCKEY and B. R. LAWN, *ibid.* **10** (1975) 1275.
71. C. GURNEY and S. PEARSON, *Proc. R. Soc.* **A192** (1948) 537.
72. A. G. EVANS and E. R. FULLER, *Metall. Trans.* **5** (1974) 27.
73. A. G. EVANS, L. R. RUSSEL and D. W. RICHERSON, *ibid.* **6A** (1975) 707.
74. Y. W. MAI, A. G. ATKINS, *ibid.* **6A** (1975) 2161.
75. R. J. STOKES, T. L. JOHNSTON and C. H. LI, *Trans. AIME* **218** (1960) 655.
76. A. R. C. WESTWOOD, *Ind. Eng. Chem.* **56** (1964) 15.
77. A. J. HOLLAND and W. E. S. TURNER, *J. Soc. Glass Technol.* **21** (1937) 383.
78. T. C. BAKER and F. W. PRESTON, *J. Appl. Phys.* **17** (1946) 179.
79. R. E. MOULD, *J. Amer. Ceram. Soc.* **43** (1960) 160.
80. B. A. PROCTOR, *Phys. Chem. Glasses* **3** (1962) 7.
81. R. H. DOREMUS and E. K. PAVELCHEK, *J. Appl. Phys.* **46** (1975) 4096.
82. T. P. DABBS and B. R. LAWN, *J. Amer. Ceram. Soc.* **65** (1982) C37.
83. A. G. METCALFE, M. E. GULDEN and G. K. SCHMITZ, *Glass Technol.* **12** (1971) 15.
84. A. G. METCALFE and G. K. SCHMITZ, *ibid.* **13** (1972) 5.
85. J. NAKAYAMA, *J. Amer. Ceram. Soc.* **48** (1965) 583.
86. H. G. TATTERSALL and G. TAPPIN, *J. Mater. Sci.* **1** (1966) 296.
87. R. W. DAVIDGE and G. TAPPIN, *ibid.* **3** (1968) 165.
88. J. NAKAYAMA, H. ABE and R. C. BRADT, *J. Amer. Ceram. Soc.* **64** (1981) 671.
89. J. P. BERRY, *Nature* **185** (1960) 91.
90. G. P. MARSHALL, L. H. COUTTS and J. G. WILLIAMS, *J. Mater. Sci.* **9** (1974) 1409.
91. W. DÖLL and G. W. WEIDMAN, *ibid.* **11** (1976) 2348.
92. R. D. MARGOLIS, R. W. DUNLAP and H. MARKOVITZ, ASTM STP 601 (American Society for Testing and Materials, Philadelphia, 1976) p. 391.
93. H. S. DOBBS, J. E. FIELD and A. H. MAITLAND, *Phil. Mag.* **28** (1973) 33.
94. A. I. BAILEY, *J. Appl. Phys.* **32** (1961) 1407.
95. H. DANNENBERG, *J. Appl. Polym. Sci.* **5** (1961) 125.
96. L. J. BROUTMAN and F. J. McGARRY, *ibid.* **9** (1965) 589.
97. R. S. RIVLIN, *Paint Technol.* **9** (1944) 215.
98. B. V. DERYAGIN and N. A. KROTOVA, *Dokl. Akad. Nauk SSSR* **61** (1948) 849.
99. D. W. AUBREY, "Adhesion 3", edited by K. W. Allen (Applied Science, London, 1978) p. 191.
100. D. W. AUBREY and M. SHERRIFF, *J. Polym. Sci.* **18** (1980) 2597.
101. S. YAMINI and R. J. YOUNG, *Polymer* **18** (1977) 1075.
102. R. J. YOUNG and P. W. R. BEAUMONT, *J. Mater. Sci.* **11** (1976) 776.
103. S. YAMINI and R. J. YOUNG, *ibid.* **14** (1979) 1609.
104. S. MOSTOVOY, P. B. CROSLEY and E. J. RIPLING, ASTM STP 601 (American Society for Testing and Materials, Philadelphia, 1976) p. 234.
105. W. L. FOURNEY and T. KOYBAYASHI, ASTM STP 678 (American Society for Testing and Materials, Philadelphia, 1979) p. 47.
106. T. K. M. WONG, PhD Thesis, Council for National Academic Awards, London (1969).
107. A. K. GREEN and P. L. PRATT, *Eng. Fract. Mech.* **6** (1974) 71.
108. L. J. BROUTMAN and T. KOBAYASHI, "Dynamic crack propagation", edited by G. C. Sih (Noordhoff, Leyden, 1973) pp. 215–25.
109. J. A. KIES, A. M. SULLIVAN and G. R. IRWIN, *J. Appl. Phys.* **21** (1950) 716.
110. A. SMEKAL, *Glasstechn. Ber.* **23** (1950) 186.
111. B. COTTERELL, *Int. J. Fract. Mech.* **4** (1968) 209.
112. F. A. JOHNSON and J. C. RADON, *Eng. Fract. Mech.* **4** (1972) 555.
113. J. G. WILLIAMS. *Int. J. Fract.* **8** (1972) 393.
114. D. W. AUBREY, G. N. WELDING and T. WONG, *J. Appl. Polym. Sci.* **13** (1969) 2193.
115. J. J. BENBOW, *Proc. Phys. Soc.* **78** (1961) 970.
116. M. I. HAKEEM and M. G. PHILLIPS, *J. Mater. Sci.* **13** (1978) 2284.
117. *Idem, ibid.* **14** (1979) 2901.
118. Y. W. MAI, *J. Mater. Sci.* **10** (1975) 943.
119. B. W. CHERRY and K. W. THOMSON, *ibid.* **14** (1979) 3004.
120. J. R. VARNER and V. D. FRECHETTE, *J. Appl. Phys.* **42** (1971) 1983.
121. T. A. MICHALSKE, J. R. VARNER and V. D. FRECHETTE, "Fracture mechanics of ceramics", Vol. 4, edited by R. C. Brandt, D. P. H. Hasselman and F. F. Lange (Plenum, New York, 1978) p. 639.
122. T. A. MICHALSKE and V. D. FRECHETTE, *J. Amer. Ceram. Soc.* **63** (1980) 603.
123. S. J. BURNS and B. R. LAWN, *Int. J. Fract. Mech.* **4** (1968) 339.
124. J. G. WILLIAMS and G. P. MARSHALL, *Proc. R. Soc.* **A342** (1975) 55.
125. P. CHANTIKUL, B. R. LAWN, H. RICHTER and S. W. FREIMAN, *J. Amer. Ceram. Soc.* **66** (1983) 515.
126. N. PERRONE and H. LIEBOWITZ, Proceedings

of the 1st Conference on Fracture, Vol. 3, Sendai, Japan, edited by T. Yokobori, T. Kawasaki, J. L. Swedlow, (Japanese Society for Strength and Fracture of Materials, 1966) p. 2065.
127. J. NEWMAN and W. H. SMYRL, *Metall. Trans.* **5** (1974) 469.
128. L. R. F. ROSE, *Int. J. Fract.* **17** (1981) 45.
129. A. G. EVANS and M. LINZER, *J. Amer. Ceram. Soc.* **56** (1973) 575.
130. A. G. EVANS, M. LINZER and L. R. RUSSEL, *Mater. Sci. Eng.* **15** (1974) 253.
131. J. S. NADEAU, *J. Amer. Ceram. Soc.* **64** (1981) 585.
132. W. E. SWINDLEHURST and T. R. WILSHAW, *J. Mater. Sci.* **11** (1976) 1653.
133. R. MOUGINOT and D. MAUGIS, *ibid.* in press.
134. L. S. BRYUKHANOVA, I. A. ANDREEVA and V. I. LIKHMAN, *Sov. Phys. Solid State* **3** (1962) 2025.
135. A. R. C. WESTWOOD and M. H. KAMDAR, *Philos. Mag.* **8** (1963) 787.
136. K. KAMDAR, *Progr. Mater. Sci.* **15** (1973) 289.
137. N. S. STOLOFF and T. L. JOHNSTON, *Acta Metall.* **11** (1963) 251.
138. F. N. RHINES, J. A. ALEXANDER and W. F. BARCLAY, *AMS Trans.* **55** (1962) 22.
139. A. R. C. WESTWOOD, "Fracture of solids", edited by D. C. Drucker and J. J. Gilman (Interscience, New York, 1963) p. 553.
140. A. K. HUNTINGTON, *J. Inst. Metals* **11** (1914) 108.
141. E. HEYN, *ibid.* **12** (1914) 3.
142. P. A. REHBINDER and E. D. SHCHUKIN, "Progress in Surface Science", Vol. 3, Part 2 (Pergamon, Oxford, 1972) pp. 97–188.
143. *Idem, Sov. Phys. Uspekki* (1973) 533.
144. D. MAUGIS and G. ANDARELLI, *Metaux, Corrosion, Industrie* No. 581 (1974) 19.
145. *Idem, ibid.* No. 583 (1974) 119.
146. *Idem, ibid.* No. 584 (1974) 167.
147. E. D. SHCHUKIN, "Surface effects in crystal plasticity," edited by R. M. Latanision and J. T. Fourie (Noordhoff, Leyden, 1977) p. 701.
148. V. I. LIKHTMAN and E. D. SHCHUKIN, *Sov. Phys. Uspekhi* **66** (1958) 91.
149. W. ROSTOKER, J. M. McCAUGHEY and H. MARKUS, "Embrittlement by liquid metals" (Rheinhold, New York, 1960).
150. V. I. LIKHTMAN, E. D. SHCHUKIN and P. A. REHBINDER, "Physicochemical mechanics of Metals" (Israel Program for Scientific Translation, Jerusalem, 1964).
151. N. S. STOLOFF, R. G. DAVIES and T. L. JOHNSTON, "Environment sensitive mechanical behavior", edited by A. R. C. Westwood and N. S. Stoloff (Gordon and Breach, New York, 1966) p. 613.
152. N. S. STOLOFF, "Surfaces and Interfaces", Vol. 2, edited by J. J. Burke, N. L. Read and V. Weiss (Syracuse University, Syracuse, New York, 1968) p. 157.
153. A. R. C. WESTWOOD, C. M. PREECE and M. H. KAMDAR, "Fracture", Vol. 3, edited by H. Liebowitz (Academic Press, New York, 1971) p. 589.
154. M. G. NICHOLAS and C. F. OLD, *J. Mater. Sci.* **14** (1979) 1.
155. S. P. LYNCH, "Advances in the Mechanics and Physics of Solids", Vol. 2, edited by R. M. Latanision and T. E. Fisher (Harwood Academic, Chur, London, New York, Paris, Utrecht, 1983) p. 265.
156. J. R. LOW, *Trans. AIME* **245** (1969) 2481.
157. M. P. SEAH, *Surf. Sci.* **53** (1975) 168.
158. *Idem, Proc. R. Soc.* **A349** (1976) 535.
159. *Idem, Acta Metall.* **25** (1977) 345.
160. M. P. SEAH and E. D. HONDROS, "Atomistics of fracture", edited by R. M. Latanision and J. R. Pickens (Plenum, New York, 1983) p. 855.
161. A. G. SKVORTSOV, G. A. SINEVITCH, N. V. PERTSOV, E. D. SHCHUKIN and P. A. REHBINDER, *Sov. Phys. Dokl.* **15** (1971) 669.
162. D. MAUGIS and G ANDARELLI, *J. Appl. Phys.* **43** (1972) 4258.
163. R. DEFAY, I. PRIGOGINE and A. BELLEMANS, "Surface tension and adsorption" (Longmans, London, 1966) p. 94.
164. A. W. ADAMSON, "Physical chemistry of surfaces" (Wiley, New York, 1976) p. 389.
165. D. McLEAN, "Grain boundaries in metals" (Clarendon, Oxford, 1957) p. 299.
166. C. LEA and M. P. SEAH, *Philos. Mag.* **35** (1977) 213.
167. E. D. HONDROS and M. P. SEAH, *Metall. Trans.* **8A** (1977) 1363.
168. E. D. HONDROS, *Proc. R. Soc.* **A286** (1965) 479.
169. M. P. SEAH and E. D. HONDROS, *ibid.* **A335** (1973) 191.
170. E. D. HONDROS and D. McLEAN, *Philos. Mag.* **29** (1974) 771.
171. M. C. INMAN and H. R. TIPLER, *Metall. Rev.* **8** (1963) 105.
172. J. P. HIRTH and J. R. RICE, *Metall. Trans.* **11A** (1980) 1501.
173. M. P. SEAH, *Acta Metall.* **28** (1980) 955.
174. A. A. GRIFFITH, *Phil. Trans. R. Soc.* **A221** (1920) 163.
175. E. OROWAN, *Trans. Inst. Eng. Shipbldrs. Scotl.* **89** (1945) 165.
176. G. R. IRWIN and J. A. KIES. *Weld. J. Res. Suppl.* **31** (1952) 95.
177. *Idem, ibid.* **33** (1954) 193.
178. H. H. WESTERGAARD, *Trans. ASME* **61** (1939) A49.
179. I. N. SNEDDON, *Proc. R. Soc.* **187** (1946) 229.
180. G. R. IRWIN, *J. Appl. Mech.* **24** (1957) 361.
181. G. R. IRWIN, "Encyclodedia of Physics", Vol. 7, edited by Flügge (Springer Verlag, 1958).
182. E. OROWAN, *Rep. Progr. Phys.* **12** (1949) 185.
183. G. R. IRWIN, *Trans. ASM* **40A** (1948) 147.
184. J. E. STRAWLEY and W. F. BROWN, ASTM STP 381 (American Society for Testing and Materials, Philadelphia, 1965) p. 133.
185. G. R. IRWIN and P. C. PARIS, "Fracture", Vol. 3, edited by H. Liebowitz (Academic, New York,

1971) p. 1.
186. J. R. RICE, Proceedings of 1st International Congress on Fracture, Vol. 1, Sendai, Japan, 1965, edited by T. Yokobori, T. Kawasaki and J. L. Swedlow, (Japanese Society for Strength and Fracture of Materials, 1966) p. 2065.
187. C. J. McMAHON and V. VITEK, *Acta Metall.* **27** (1979) 507.
188. M. L. JOKL, V. VITEK and C. J. McMAHON, *Acta Metall.* **28** (1980) 1479.

Received 16 July
and accepted 4 December 1984